

65/16

TECHNICAL NOTE RL-243

TECHNICAL NOTE RL-243

AN EXPERIMENTAL STUDY OF THE FLOW VARIABLES AT THE MINIMUM PRESSURE STATION OF NINETY-DEGREE PIPE BENDS

by *G. R. Guinn*
G. P. Stricklin

November 1967

RESEARCH LABORATORIES

FACILITY FORM 602	N68-17429	(ACCESSION NUMBER)	(THRU)
	<u>56</u>	(PAGES)	<u>1</u>
	<u>CR-61576</u>	(NASA CR OR TMX OR AD NUMBER)	<u>10</u>
			(CATEGORY)



GPO PRICE \$ _____

CFSTI PRICE(S) \$ _____

Hard copy (HC) 3.00

Microfiche (MF) .65

BROWN ENGINEERING

A TELEDYNE COMPANY

Research Park • Huntsville, Alabama 35807

TECHNICAL NOTE RL-243

AN EXPERIMENTAL STUDY OF THE FLOW
VARIABLES AT THE MINIMUM PRESSURE
STATION OF NINETY-DEGREE PIPE BENDS

November 1967

Prepared For

PROPULSION DIVISION
PROPULSION AND VEHICLE ENGINEERING LABORATORY
GEORGE C. MARSHALL SPACE FLIGHT CENTER

By

ADVANCED SYSTEMS LABORATORIES
BROWN ENGINEERING COMPANY, INC.

Contract No. NAS8-20073

Prepared By

Dr. G. R. Guinn
G. P. Stricklin

ABSTRACT

To support liquid cavitation studies, flow variables were measured which relate to the minimum pressure in 90-degree circular pipe bends. All of the bends investigated were nominally 4 inches in diameter and had ratios of curvature radius to pipe diameter of 2.00, 1.50, 1.25, 1.00, and 0.75. Water was used as the test medium and the Reynolds number ranged from 2.5×10^5 to 1.8×10^6 . To locate the minimum wall pressure, static pressures were first measured at the inner and outer walls in the plane of curvature. The minimum wall pressure was found to occur between 22.5 degrees and 30 degrees deflection angle along the inside wall. Velocity and pressure traverses were then made across the bend at the position of minimum pressure. The total pressure was found to be roughly uniform in the central core and the velocity profile was found to correspond generally to that for free vortex flow. It was found that minimum pressures in the bend could be approximated by free vortex flow; however, the predicted values will be conservative, e.g., low, when viewed from the standpoint of cavitation.

Approved:

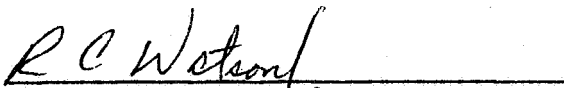


Dr. E. J. Rodgers

Manager

Mechanics and Thermodynamics Department

Approved:



R. C. Watson, Jr.

Vice President

TABLE OF CONTENTS

	Page
INTRODUCTION	1
DISCUSSION	4
Apparatus	7
Procedure	16
ANALYSIS	20
RESULTS	23
CONCLUSIONS	44
REFERENCES	46

LIST OF FIGURES

<u>Figure</u>		<u>Page</u>
1	Schematic of the Pressure Distribution on the Inner and Outer Walls in the Plane of Curvature of an Elbow	5
2a	Photograph of the Test Facility Used in the Experimental Investigations	8
2b	Schematic of the Test Facility Used in the Experimental Investigations	9
3a	Schematic of the Elbow Test Section for Wall Pressure Measurements	11
3b	Schematic of the Elbow Test Section for Traverse Measurements	13
4a	Schematic of the Kiel Probe for Measuring Total Pressure	15
4b	Schematic of the Prism Probe for Measuring Velocity Vector, Total Pressure and Static Pressure	15
5	Velocity Traverse Upstream of Bend Compared with 1/8 Velocity Profile ($R/2a = 0.75$)	24
6	Variation of Minimum Wall Pressure Coefficient with Reynolds Number	26
7	Variation of the Wall Pressure Coefficient with Reynolds Number ($R/2a = 0.75$)	27
8a	Variation of Wall Pressure Coefficient with Distance Along Bend Centerline ($R/2a = 2.00$)	28
8b	Variation of Wall Pressure Coefficient with Distance Along Bend Centerline ($R/2a = 1.50$)	29
8c	Variation of Wall Pressure Coefficient with Distance Along Bend Centerline ($R/2a = 1.25$)	30
8d	Variation of Wall Pressure Coefficient with Distance Along Bend Centerline ($R/2a = 1.00$)	31

LIST OF FIGURES - Concluded

<u>Figure</u>		<u>Page</u>
8e	Variation of Wall Pressure Coefficient with Distance Along Bend Centerline ($R/2a = 0.75$)	32
9a	Experimental Results from Probe Traverses ($R/2a = 2.00$, $\theta_{\min} = 22\frac{1}{2}^\circ$)	34
9b	Experimental Results from Probe Traverses ($R/2a = 1.50$, $\theta_{\min} = 22\frac{1}{2}^\circ$)	35
9c	Experimental Results from Probe Traverses ($R/2a = 1.25$, $\theta_{\min} = 30^\circ$)	36
9d	Experimental Results from Probe Traverses ($R/2a = 1.00$, $\theta_{\min} = 30^\circ$)	37
10	Flow Pitch Angles Measured Relative to a Tangent To the Bend Centerline	40
11	Comparison of Measured Minimum Wall Pressure Coefficient with Potential Flow Theory	41
12	Variation of C_{wall} with Radius of Curvature, R'	42

LIST OF SYMBOLS

A	Cross-sectional area of the pipe bend
a	Pipe radius
C	Constant defined by Equation 9
C_p	Pressure coefficient
f	Signal frequency from the flow meter or calibrator in hertz
h	Static pressure head in inches of Mercury
K_1', K_2'	Constants related to the free vortex motion in the central core
P	Total pressure
p	Static pressure
Q	Flow rate in gallons per minute
R'	Radius of curvature of pipe bend nondimensionalized by a
Re	Pipe Reynolds number = $\left(\frac{2\rho \bar{W}a}{\mu} \right)$
r	Radial distance from pipe centerline nondimensionalized by a
\bar{W}	Average axial velocity through the pipe
W_1'	Central core velocity immediately upstream of the bend nondimensionalized by \bar{W}
$\delta_{2,0}'$	Boundary layer thickness at the inside wall nondimensionalized by a
θ_{\min}	Deflection angle at which the wall pressure is a minimum
μ	Dynamic viscosity
ρ	Liquid density
() ₁	Refers to uniform conditions immediately upstream of the bend
() ₀	Refers to conditions at the edge of the viscous layer

LIST OF SYMBOLS (Continued)

$\overline{(\)}$	Average
$(\)_{\text{ref}}$	Reference condition
$(\)_{\text{wall}}$	Refers to conditions at the wall
$(\)_{\text{min}}$	Minimum
$(\)_{\text{core}}$	Refers to conditions at the edge of the central core
$(\)_{\text{L}}$	Refers to condition at the bend centerline
$(\)_{\text{T}}$	Total or stagnation condition

INTRODUCTION

The flow of fluids in pipe bends has been a topic of practical consideration for a number of years. A recent and largely unexplored region of interest in curved pipe flow has evolved around the ducting of the liquids which are employed as the propellants for liquid rocket engines. With these liquids there may arise the undesirable phenomenon of liquid cavitation near the inside wall of pipe bends that are located in the ducting system on the suction side of the turbopumps.

The presence of cavitation in these components can have a number of detrimental effects on the overall design and performance of the propulsion system. Because of the hysteresis effects associated with the formation and disappearance of cavitation bubbles, the vaporous pockets formed in a cavitating pipe bend may persist in a supercooled state for some distance downstream before collapse. These bubbles form "weak spots" in the liquid and, if they are convected downstream into a pump, they can provide the nuclei for premature inception of cavitation within the pump itself. Once this happens, the formation and collapse of the bubbles markedly degrades pump efficiency and induces undesirable pressure fluctuations which can be transmitted to the rocket engine combustion chamber.

To suppress cavitation within the pump, it is necessary to bring the liquid to the inlet section under a sufficient "net positive suction head" (NPSH) defined as the total pressure at the pump inlet minus the vapor pressure of the propellant at the pump inlet. The required inlet pressure may be obtained either by auxiliary pumps or by pressurization of the propellant tanks. The tank pressure that would be required is

$$P_{\text{tank}} = \text{NPSH} + \text{feedline friction loss} \\ + \text{vapor pressure} - \text{propellant head.}$$

The NPSH in the equation above is that at which the pump is known to operate satisfactorily, and its value will increase if the upstream ducting components, in this case the pipe bends, alter the conditions at the pump inlet from the ideal conditions presupposed for design purposes. Therefore, through the above relationship, the cavitation of pipe bends located on the suction side of the turbopumps can directly influence the required pump inlet pressure along with the objectional weight penalties associated with the auxiliary pressurization components. For this reason it is desirable to design the propellant pumps and the ancillary ducting components so that the lowest pressure possible is required at the pump inlet to assure cavitation free operation. Considerable effort has been devoted to the design of pumps¹⁻⁶ so that the NPSH required for proper operation is minimized; however, the influence of the upstream ducting components (pipe bends) on cavitation within the pump has not been adequately determined nor has there been any effort, beyond the exploratory phase, expended in achieving an understanding of the cavitation characteristics of flow in curved pipes.⁷

A number of factors are known to affect the inception of cavitation; however, their relationships to each other and the manner in which they exercise their influence on the cavitation process are not altogether known with any degree of certainty.⁸⁻¹² Therefore, the investigation of the cavitation characteristics of any hydraulic device eventually involves the full scale experimental determination of these effects. Fortunately most of these factors exercise only a small influence on the inception of cavitation and then in a manner which usually results in a conservative hydrodynamic design when it is desirable to operate free of cavitation. As one would intuitively reason, the minimum static pressure sustained in a ducting component and the vapor pressure of the liquid are the two most important factors influencing the conditions at which cavitation first appears. Hence if a specified liquid is to be employed, a knowledge of the minimum pressure intensity occurring in the ducting component must

at least be determined before any statements can be made regarding the probability of cavitation.

To provide some understanding of the flow processes that relate to the minimum pressure in a circular pipe bend, a program was initiated at Brown Engineering Company which included both analytical and experimental studies. A literature survey is contained in Reference 7 and the results of the analytical study are contained in Reference 13. It is the purpose of this report to summarize the results of the experimental program, some of which have already been reported in Reference 14.

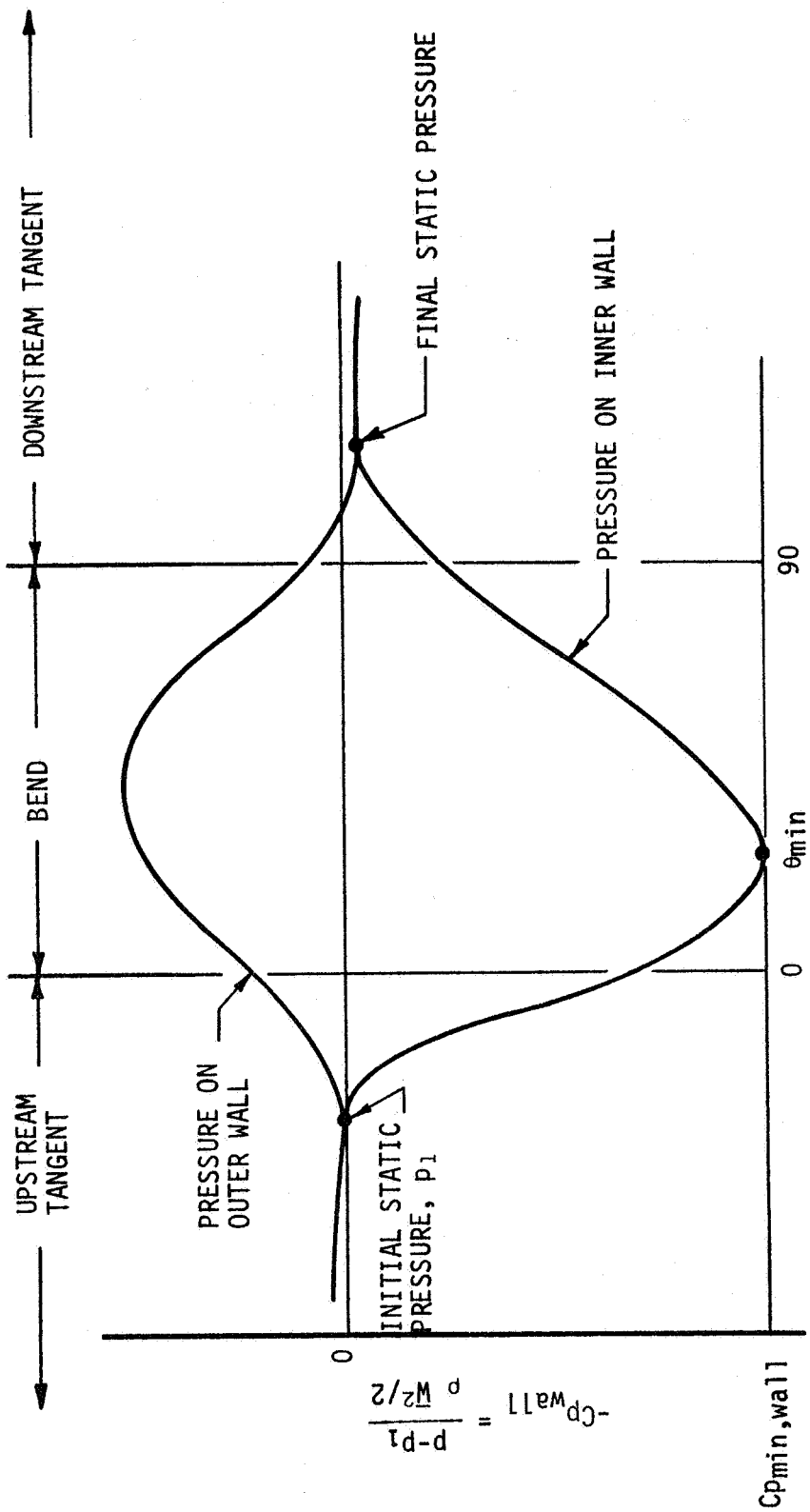
DISCUSSION

Experimentation on curved pipes has in the past emphasized primarily the losses associated with turning the flow since it has traditionally been of major significance in hydraulic designs. Experimental studies of the pressures have been rather limited in scope, although pipe bends have some utility as flow meters, with the pressure differential between the inside and the outside walls as the flow rate indication.¹⁵⁻¹⁷

Figure 1 is a general schematic of the wall pressures that one may expect in the plane of curvature of a finite deflection angle pipe bend. Such a profile is characteristic of curved rectangular channels as well as the circular cross-section bends which are considered herein.

The pressure difference across a bend is generated in order to balance the centrifugal forces acting upon the fluid particles which are following curved paths. The pressure at the outside of the bend increases above the initial static pressure and the pressure at the inside decreases from its initial value until some minimum value is reached. Thus, as the flow undergoes the transition from rectilinear to curvilinear motion, a positive pressure gradient in the direction of flow is initially imposed on the outer wall of the elbow and then a negative gradient is generated as the static pressure readjusts to a uniform value when the flow leaves the bend. Conversely, on the inner wall, a negative axial pressure gradient is initially formed and is followed by a positive gradient as the pressure increases back to a uniform value across the duct downstream of the turn.

When the turning radius is sharp and the flow rates high, the centrifugal forces acting on the flow are large and hence the positive axial pressure gradients may be of sufficient magnitude and extent so that the slow moving fluid particles near the wall lack sufficient momentum to traverse the region of increasing pressure. If this is the case, the particles will reverse their original direction of motion and create a local region of eddies and vortexing near the duct boundaries. That is, the main flow fails to adhere to the walls of the duct or it "separates", a very



BEND DEFLECTION ANGLE, θ - deg

Figure 1. Schematic of the Pressure Distribution on the Inner and Outer Walls in the Plane of Curvature of an Elbow

undesirable phenomenon since energy losses which accentuate the resistance to flow are created by the vortexing action of separation.

Inside the pipe bend away from the walls, the pressure is primarily governed by the inviscid momentum balance on the particles moving in curvilinear paths. For fully developed turbulent flow at the bend entrance, this balance is approximately that which occurs for potential flow if the location considered is not too far from the bend entrance. Near the wall, however, the profile becomes distorted by the viscous effects present there. These effects are such that the minimum pressure in a bend cross sectional plane could occur at some distance, $\delta_{2,0}$, from the inside wall rather than immediately adjacent to it.¹⁸

If the fluid is a liquid with a sufficiently high vapor pressure, the static pressure near the inside wall of the duct may depress to a value equal to or less than the vapor pressure and thus cause cavitation within the elbow. This is an entirely different phenomenon from separation, although both may occur simultaneously.

The analysis performed in Reference 13 was an attempt to predict the minimum pressure in a circular pipe bend using the shedding layer concept with a potential central core. Restrictions on the analysis precluded the ability to predict the deflection angle at which the minimum pressure occurs and the ability to predict accurate boundary layer thickness. The former restriction is not a severe limitation because this information is not vital to the study of the cavitation characteristics. The latter restriction affects the results in a conservative manner when one is concerned with cavitation, e. g., the predicted values of minimum pressure are lower than those actually achieved.

The purpose of the initial investigation is to obtain the static pressure profiles in the plane of curvature of 90-degree circular pipe bends. Of primary concern is the determination of the minimum pressure at the wall and the deflection angle at which it occurs. The second phase of the

experimental program consists of pressure and velocity traverses across the bends along a line determined by the intersection of the plane of curvature and a cross sectional plane located at the deflection angle of minimum pressure, θ_{\min} . It is expected that the results of these investigations will help in acquiring a better understanding of curved pipe flow in the transition region and will become the basis for future studies of bend cavitation and for establishing the utility of curved pipe analyses in the transition region.

The present investigation was conducted using water as the fluid medium. A range of Reynolds numbers, based on pipe diameter, was studied with 1.8×10^6 being the maximum and 2.5×10^5 being the minimum. Five bend radii of curvatures were investigated, namely, 2.00, 1.50, 1.25, and 0.75 times the inside diameter, which was nominally 4 inches.

APPARATUS

General Description

The facility (Figure 2a) used in this study is a constant diameter closed return loop oriented in the vertical plane and using water as the test medium. The elbow test sections form the second bend in the upper limb of the test loop (Figure 2b) which is primarily fabricated from 4-inch-diameter heavy wall copper tubing (Type L) with standard bronze sweat solder elbows and 150-pound flanges. To insure the attainment of fully developed turbulent flow at the test bend entrance, the elbow test sections are connected on the upstream side to a straight pipe run which is 60 diameters long and is preceded by a flow straightener. To minimize the transmission of vibrations to the test sections, flexible metal hoses form the portion of the loop immediately adjacent to the control valve and the pump. Also the pipe sections are insulated from the supports with rubber padding. A 62-gallon accumulator tank is provided to impose additional hydrostatic head on the system and to absorb spurious pressure surges

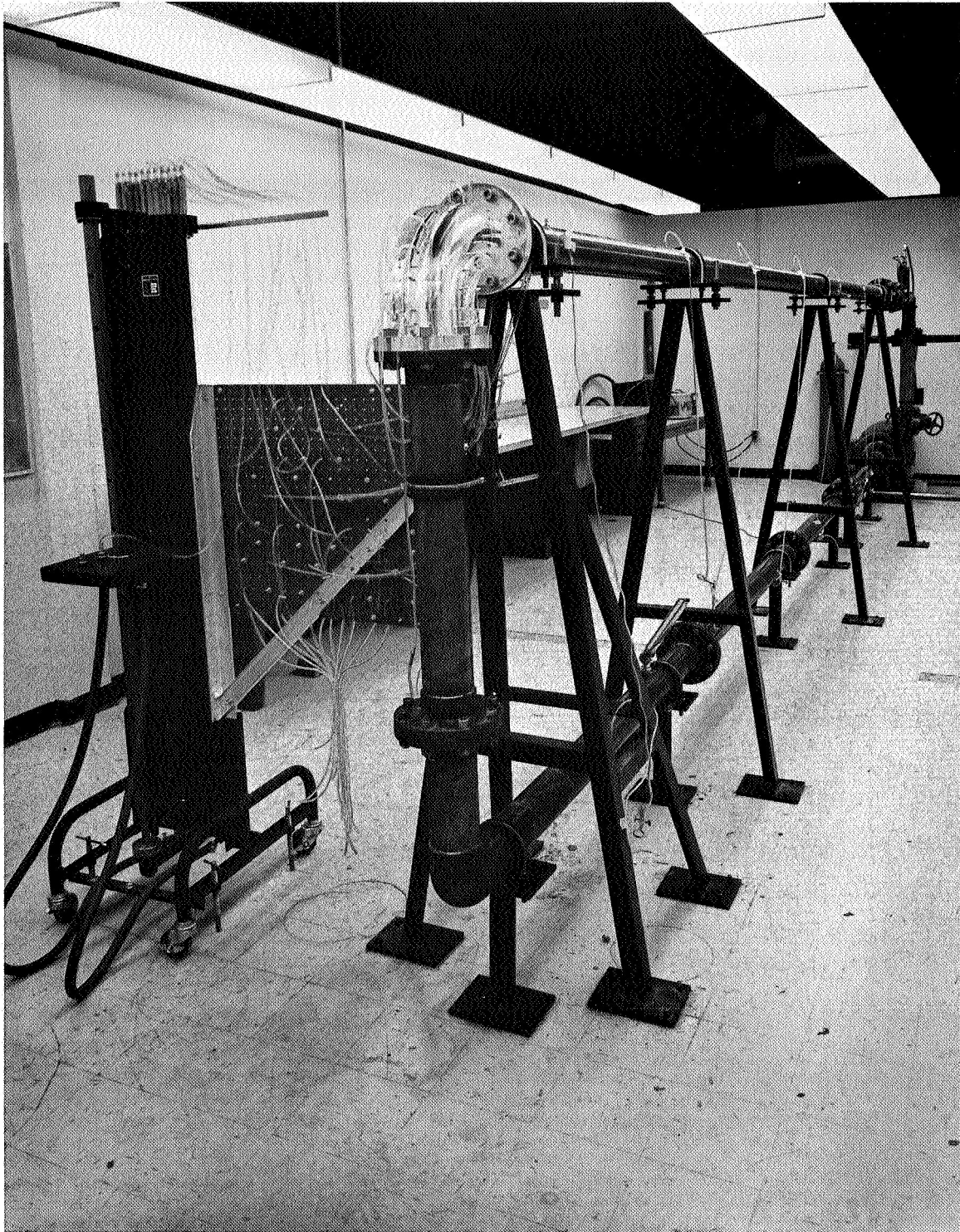


Figure 2a. Photograph of the Test Facility Used in the Experimental Investigations

in the test loop. To remove part of the dissolved air, the water from the utility line is used to impose a mild vacuum in the ullage. Control of the flow rate through the system is achieved by regulating the pressure drop with a gate valve mounted to the outlet side of the pump.

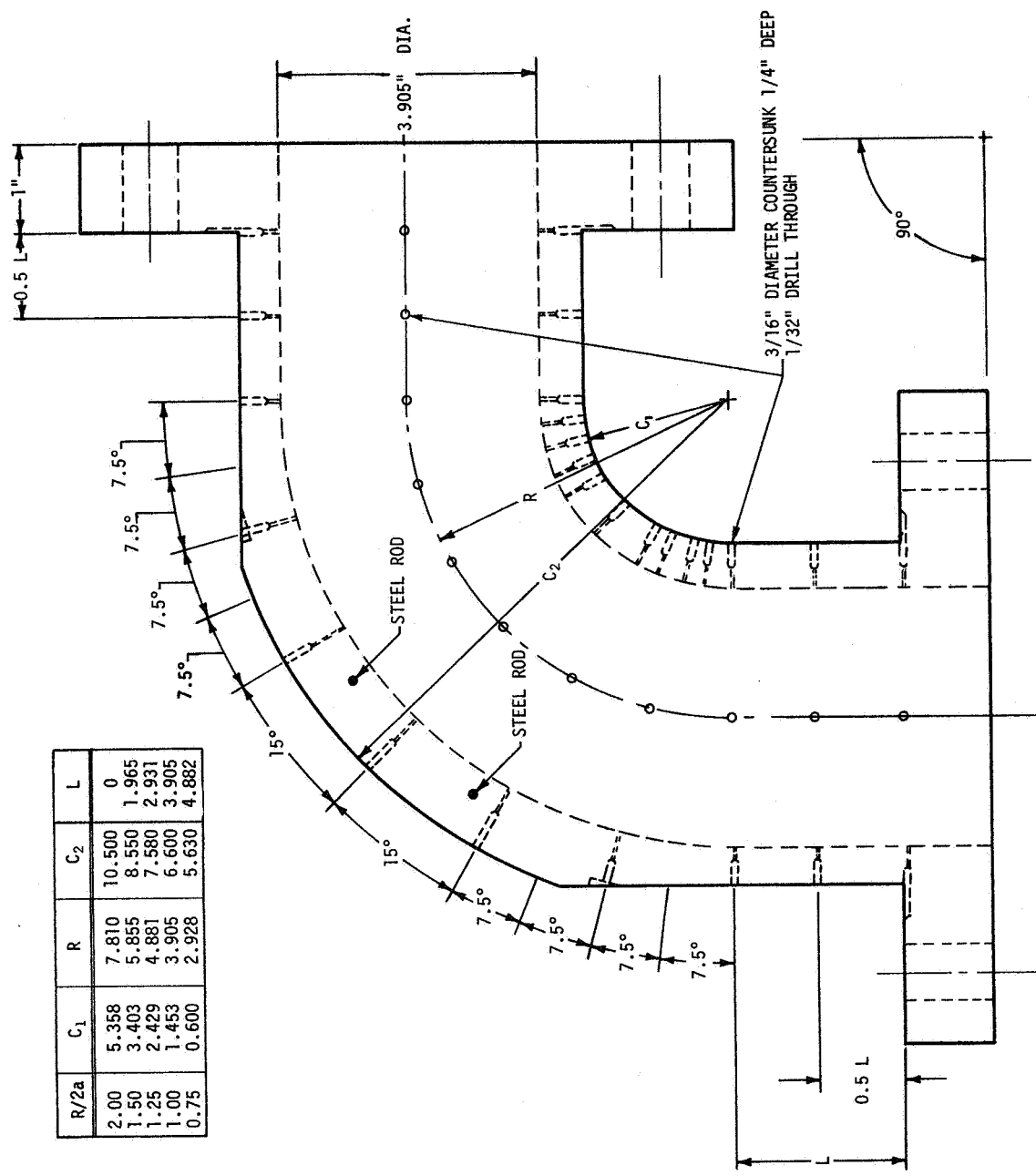
The loop is driven by a commercially available close coupled pump which was selected to achieve minimal vibration associated with shaft misalignment. Design rating of the pump is 1100 gal/min with a total head rise of 150 feet of liquid at 1770 rpm. The pump is powered by a 60 horsepower, 440 volt, three-phase motor. The ultimate Reynolds number with the present components is about 1.8×10^6 .

Test Sections

Five different elbow test sections were used in the present investigation. The radii of centerline curvature were 2.00, 1.50, 1.25, 1.00 and 0.75 times the internal diameter.

The test sections were fabricated from transparent acrylic plastic. The internal contour of each elbow was accurately machined into two plastic sheets of appropriate thickness. The two halves were then bonded together with an epoxy cement to form a pipe bend with the seam in the plane of curvature. Flanges were then bonded to the ends of the curved section. The surfaces were polished to approximately 10 rms finish so that the flow could be visually observed.

Instrumentation of the test bends for wall pressure measurements consisted of a number of static pressure taps as illustrated in Figure 3a. The taps were formed by drilling 3/16-inch holes to within 1/4 inch of the inside wall and then drilling through the surface with a 1/32-inch-diameter drill. The taps at the flanges were not drilled but were formed by milling 0.016-inch deep circular grooves into the parts before assembly. Wires of 0.032-inch diameter were coated with a mould release and positioned in the grooves before the ports were cemented together. After the parts were cemented together, these wires were then removed when the cement



R/2a	C ₁	R	C ₂	L
2.00	5.358	7.810	10.500	0
1.50	3.403	5.855	8.550	1.965
1.25	2.429	4.881	7.580	2.931
1.00	1.453	3.905	6.600	3.905
0.75	0.600	2.928	5.630	4.882

Figure 3a. Schematic of the Elbow Test Section For Wall Pressure Measurements

had set. The openings were carefully hand polished to remove burrs and imperfections which could affect the accuracy of the measured results. Brass connectors with a 3/32-inch straight thread on one end and 1/16-inch hose fitting on the other were cemented into the taps in the bend. Where space was limited at the inside of some of the small curvature bends, a 1/16-inch countersink was used and 1/16-inch-diameter copper tubing was employed as hose connectors.

The traversing probes were mounted in the bends through 1/8-inch-diameter holes (Figure 3b) located on the inner and outer walls at the deflection angles of either 22-1/2 degrees or 30 degrees. The probe stems were clamped in manual traversing units which permitted vernier measurement of the immersion depth. A vernier for probe rotation was also provided which permitted nulling the yaw angle relative to the axis of the sensing head.

Instrumentation

Test section pressures were measured by a Meriam 10-tube manometer with a 60-inch range. All measurements were made with mercury as the indicating fluid and were referenced to a static pressure tap upstream of the test section. Piezometer lines were of transparent plastic tubing which were connected to the test section through a series of valves used to bleed off trapped air bubbles. Pressure data were recorded on 2- by 3-inch lantern slides with a tripod mounted Polaroid camera. The slides were then projected onto a screen which permitted readings of the pressure differences to within approximately ± 0.02 inches of mercury. The mercury was periodically removed from the manometer and was cleaned by filtering three times through 50 percent dilute nitric acid. The manometer was cleaned with detergent and water followed by an acetone rinse; the glass tubes were cleaned with bichromate acid.

Flow rates through the loop are measured with a propeller-type volumetric flowmeter (Pottermeter) located in the 4-inch-diameter line

$R/2a$	θ_{min}
2.00	22.5°
1.50	22.5°
1.25	30.0°
1.00	30.0°

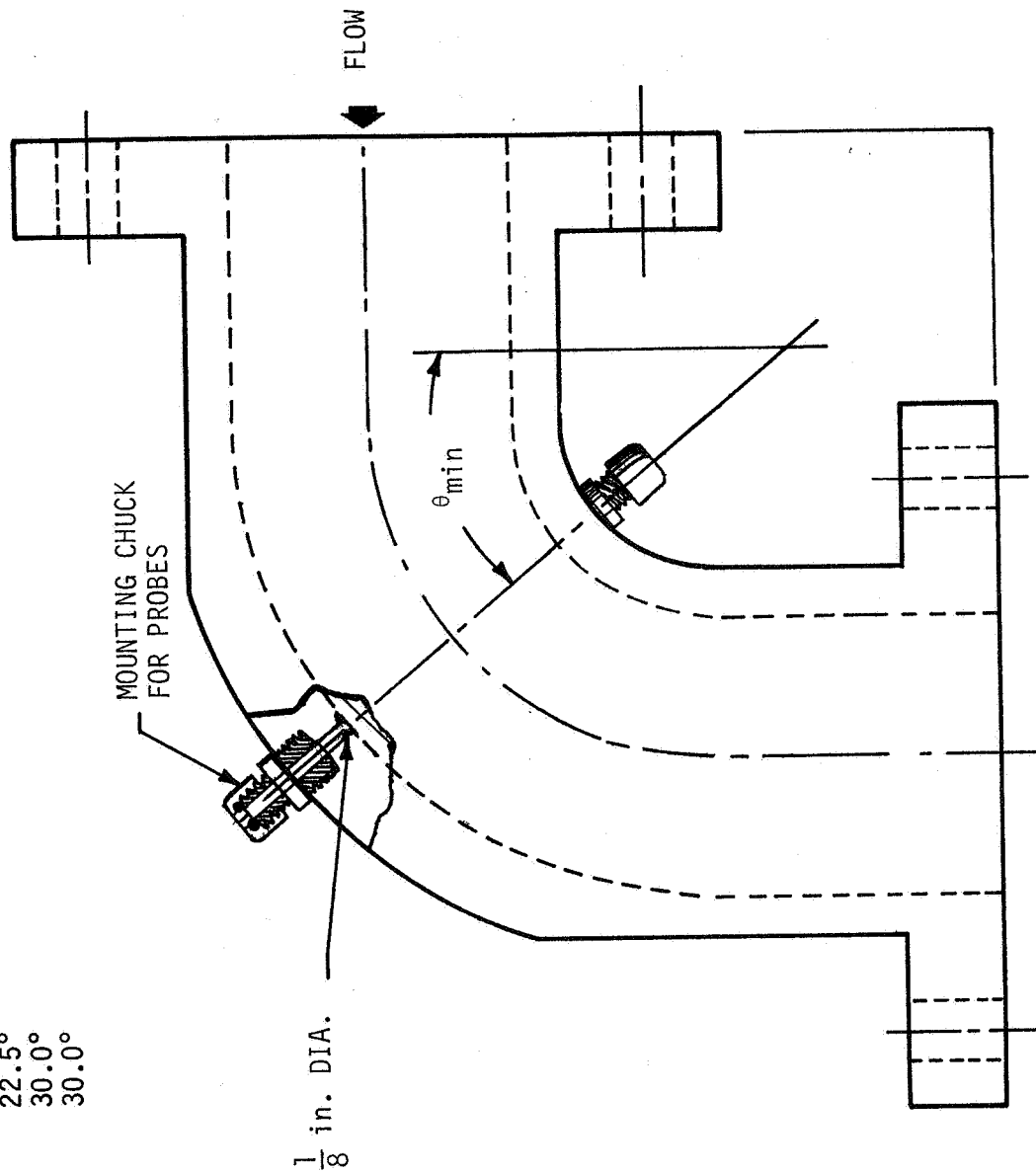


Figure 3b. Schematic of the Elbow Test Section for Traverse Measurement

on the suction side of the pump. The nominal linear range is in the interval between 75 gal/min to 1250 gal/min with a stated accuracy of ± 0.02 percent in this range. For limited operation the flowmeter can be operated at 1500 gal/min without damage to the pickup sensor. The ac signal from the flowmeter was converted to a voltage output which was recorded on a Honeywell Visicorder. The converter has a stated analog output accuracy of ± 0.1 percent. A calibration oscillator was used to calibrate the converter. The tuning fork that generates the signal has a stated accuracy of ± 0.05 percent.

The profiles across the bends were measured with two different types of probes. Traverses with Kiel probes were first made to obtain the variation of total pressure. This type of probe was chosen because it is insensitive to pitch and yaw angles up to angles of 40 degrees or more measured from the axis of the head. A sketch of the probe, made by United Sensor and Control Corporation, is shown in Figure 4a.

Velocity, static pressure and additional total pressure measurements were made with three-dimensional, directional probes with prism shaped sensing heads. With the calibration charts furnished with each probe, the five pressure indications in the sensing head yielded the aforementioned flow data as well as the flow pitch and yaw angle (which was nulled out since the probe was considered to lie on the plane of curvature). Figure 4b illustrates the three-dimensional probes, also furnished by the United Sensor Corporation.

Additional instrumentation consists of a small pressure-vacuum gage mounted on the surge tank and a well-type thermometer mounted in the 4-inch diameter line downstream of the test bend, which can be read to within about $\pm 1.0^\circ\text{F}$.

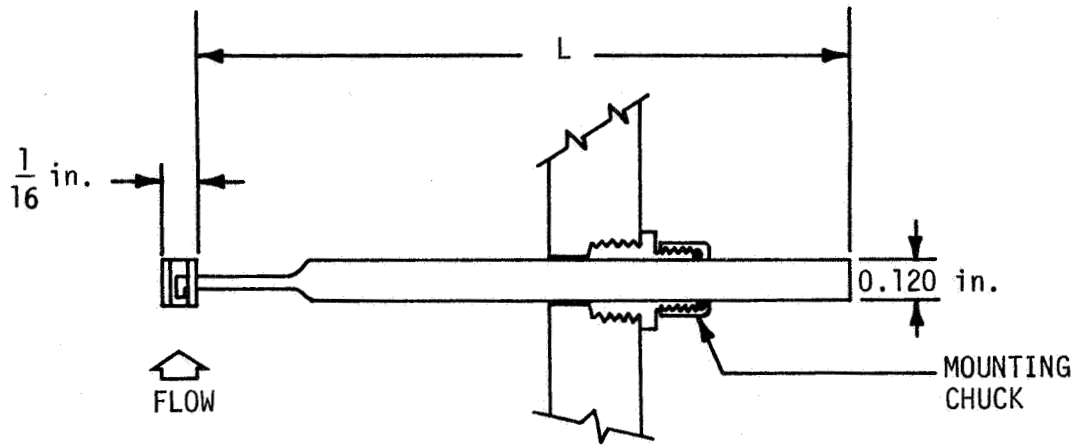


Figure 4a. Schematic of the Kiel Probe for Measuring Total Pressure

$$L = \begin{cases} 12 \text{ in. ON OUTSIDE OF BEND} \\ 16 \text{ in. ON INSIDE OF BEND} \end{cases}$$

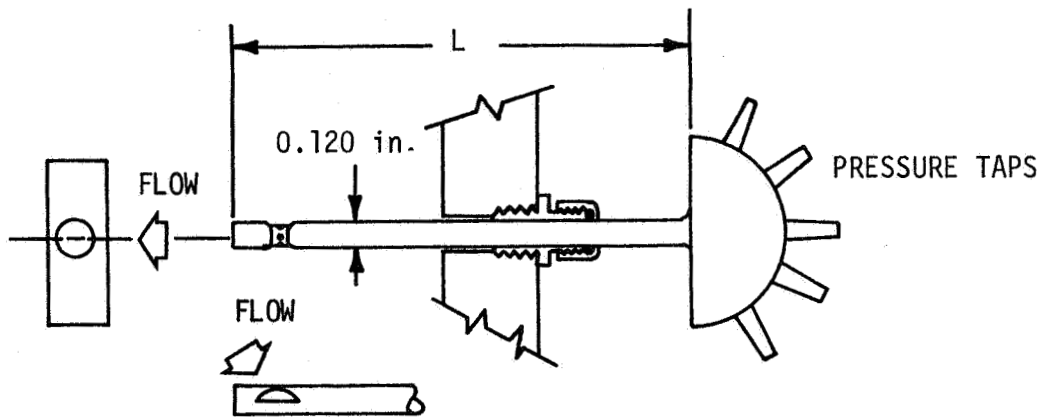


Figure 4b. Schematic of the Prism Probe for Measuring Velocity Vector, Total Pressure and Static Pressure

PROCEDURE

Facility Operation and Techniques

Untreated tap water was used as the test medium in the present study; however, before it was introduced into the system it was allowed to stand in the accumulator tank while a jet pump created a mild vacuum in the ullage. The length of time it was permitted to remain under vacuum varied from overnight to two or three days. This process sufficiently removed enough dissolved air so that the manometer lines could be bled more easily.

Before the system was filled for each run, it was thoroughly flushed with fresh tap water to remove loose scale and corrosion from the iron pump casing. The deaerated water in the surge tank was then allowed to slowly fill the loop under gravity head while air was vented from the system through the main vent, small vents on the upper leg and the pump casing vent. Thorough venting of the pump casing required rotating the impeller by hand until all trapped air was removed. The pump was then pulsed several times while the bleeding operation was intermittently performed. This procedure resulted in only a very small amount of air remaining in the system.

After filling the system the accumulator tank was partially filled with tap water and pressurized (≈ 25 psia) using the tap water pressure. The piezometer lines were then bled free of air by opening all of the manometer control valves. To bleed the lines between the valves and the manometer, the manometer well was raised to a position about 20 inches from the top of the manometer. The bleed valve and the piezometer valve of each tube were then alternately opened and closed, thus forcing the air bubbles out of the vent. This operation was repeated in turn for all manometer tubes plus the well. This procedure completely filled the piezometer connecting lines and manometer with water and removed all entrapped air from the pressure instrumentation system. The flowmeter recorder was

then calibrated using the 100, 120, 200, and 500 hertz signal generated by the calibrator.

To perform one test run, the pump motor was started with the control valve about 1/4 open and the flow rate was then adjusted to the lowest value desired (for instance, 40 percent of full flow). After the manometer indicated that equilibrium had been reached, a Polaroid picture was taken of the mercury columns and a recording was made of the temperature. The flow rate was then increased to the next highest level and the procedure repeated until the full range of flow rates had been examined for the particular elbow installed in the system. For each run it was possible to obtain wall pressure data for as many as eight flow rates before the water temperature became too great.

For the traverse measurements the two probes were positioned at the desired immersion depths relative to the inside and outside walls of the bend. After flow had been established in the loop and before any data were recorded, the heights of the two mercury columns indicating yaw were equalized by rotating the probes. Because of the slow response of the manometer with the three-dimensional probes, the number of flow rates available per run was limited to about three. During any run the water temperature ranged from room temperature to around 125°F.

The film transparencies of the pressure data were projected on a screen and then recorded. The difference between the measured pressures and the reference pressure were taken and then corrected for the weight of the additional column of water on the lower mercury column. Hence the corrected pressure difference in inches of mercury is

$$\begin{aligned}
 (h_{\text{ref}} - h)_{\text{corrected}} &= (h_{\text{ref}} - h)_{\text{measured}} - \frac{(h_{\text{ref}} - h)_{\text{measured}}}{13.56} \\
 &= 0.92625 (h_{\text{ref}} - h)_{\text{measured}} \quad (1)
 \end{aligned}$$

where 13.56 is taken as the specific gravity of mercury. The pressure data are reported in dimensionless form via a pressure coefficient defined as

$$\begin{aligned}
 C_p &= \frac{13.56 g(h_{\text{ref}} - h)_{\text{corrected}}}{\bar{W}^2 / 2} \\
 &= \frac{p_1 - p}{\rho \bar{W}^2 / 2} \quad (2)
 \end{aligned}$$

The flow variables, measured by the three-dimensional probes, were obtained from calibration charts supplied with each probe by the manufacturer. The flow rates were obtained by relating the ac signal generated by the flowmeter, to the flow rate. For the particular flowmeter used, this relationship is

$$Q = 2.882 f . \quad (3)$$

Mean velocities are obtained from the one-dimensional continuity equation

$$\bar{W} = \frac{Q}{A} \quad (4)$$

and the Reynolds number from

$$\text{Re} = \frac{2\rho\bar{W}a}{\mu} \quad (5)$$

using the viscosity data of References 26 and 27.

ANALYSIS

In the analytical portion of the investigation an attempt was made to obtain relationships for pressure and velocity based on theoretical considerations only. In order to do this it was necessary to resort to a number of important assumptions. Some of these were

- Flow in the central core* is potential.
- There is no velocity component normal to the plane of curvature in the central core.
- Viscous effects are confined to a shedding layer* adjacent to the pipe wall.

Primarily due to the boundary layer assumptions required for solution, the analysis gave inaccurate, although conservative, values of minimum pressure. The purpose of this section is to obtain some empirical relationships using the work reported in Reference 13 as a guide.

In the analytical portion of the investigation a relationship for the pressure coefficient was derived¹³ for the plane of curvature. The relationship is

$$C_p = \frac{K_1'^2 + K_2'^2}{(R' \pm r')^2} - W_1'^2 \quad (6)$$

where K_2' is approximately zero and W_1' is approximately unity. The plus sign indicates that r' is measured from the pipe centerline towards the outer wall and minus sign indicates that r' is the distance from the pipe centerline towards the inner wall. K_1' is the integration constant which is generated when the velocity profile for a potential vortex is obtained. For a curved pipe the axial velocity on the plane of curvature is¹³

*See Reference 13 for a definition.

$$W_1' = \frac{K_1'}{R_1' \pm r_1'} \quad (7)$$

K_1' can be determined by using mass flow considerations and is related to the bend radius of curvature and the average boundary layer thickness as follows

$$\frac{1}{K_1'} = 2 [R' - R'^2 - 1]^{\frac{1}{2}} + \frac{\frac{1}{4} \bar{\delta}_2' - \frac{1}{15} \bar{\delta}_2'^2}{(R'^2 - 1)^{\frac{1}{2}}} \quad (8)$$

The preceding equation can be written more conveniently as

$$\frac{1}{K_1'} = 2 [R' - (R'^2 - 1)^{\frac{1}{2}}] + \frac{C}{(R'^2 - 1)^{\frac{1}{2}}} \quad (9)$$

Now from Equations 6 and 8, the minimum pressure coefficient at the wall is

$$C_{p_{\min, \text{wall}}} = \frac{P_1 - P_{\min, \text{wall}}}{\rho \bar{W}^2 / 2} = \frac{1}{(R' - 1)^2} \left\{ 2 [R' - (R'^2 - 1)^{\frac{1}{2}}] + \frac{C_{\text{wall}}}{(R'^2 - 1)^{\frac{1}{2}}} \right\}^{-2} - W_1'^2 \quad (10)$$

where C_{wall} is a correlation coefficient which is a function of Reynolds number and radius of curvature of the bend and is to be found empirically from pressures measured at the wall. It is interesting to note the different roles of the empirical constant in the present analysis and the analysis of Addison.¹⁵ In the latter's analysis the empirical constant is a discharge coefficient multiplicative on the first term in the brackets whereas in the present analysis it is an additive term. With potential flow there are no viscous effects present and C becomes zero.

In Reference 13 an analysis of the experimental results of Weske¹⁸ indicated that K_1' is approximately equal to the dimensionless radius of curvature. If this condition is postulated, then the pressure coefficient in the central core becomes

$$C_p = \frac{R'^2}{(R' \pm r')^2} - 1 \quad (11)$$

For the approximation that K_1' equals the radius of curvature, the axial velocity is

$$W' = \frac{R'}{R' \pm r'} \quad (12)$$

It is interesting to note that these two expressions are independent of Reynolds number. The consequences of assuming that K_1' equals R' will be examined with the aid of the experimental data.

RESULTS

To determine if the velocity profile at the entrance to the bends is fully developed and is symmetric about the pipe centerline (at least in the plane coincident with the plane of curvature) a traverse was taken with the Kiel probes on the upstream straight section of the smallest radius bend. The measurements were taken along a line formed by the plane of curvature and by a plane normal to the pipe centerline and located 3-11/16 inches upstream from the start of curvature. The axial velocity profile was calculated from the measured total pressure as follows

$$\begin{aligned}\frac{W}{W_{\mathcal{L}}} &= \frac{\bar{W}}{W_{\mathcal{L}}} \left(\frac{P - P_1}{\frac{1}{2} \rho \bar{W}^2} \right)^{1/2} \\ &= \frac{\bar{W}}{W_{\mathcal{L}}} \left(C_{p_T} \right)^{1/2}\end{aligned}\quad (13)$$

From Reference 27 the ratio of average to centerline velocity is taken to be 0.837 which corresponds to a 1/8 turbulent velocity profile and a Reynolds number between 1.1×10^5 and 1.1×10^6 . Hence the axial velocity as normalized by the centerline velocity is

$$\frac{W}{W_{\mathcal{L}}} = 0.837 \left(C_{p_T} \right)^{1/2}\quad (14)$$

Figure 5 shows the values of $W/W_{\mathcal{L}}$ computed from Equation 14 and the measured C_{p_T} . A 1/8 turbulent velocity profile is also shown for comparison purposes. Since the lack of agreement between the theoretical and the experimental points is uniform, it can probably be attributed to the fact that $\bar{W}/W_{\mathcal{L}}$ is actually different from the value assumed or that p_1 in Equation 13 should be the uniform static pressure at the measuring station rather than that at the reference station slightly

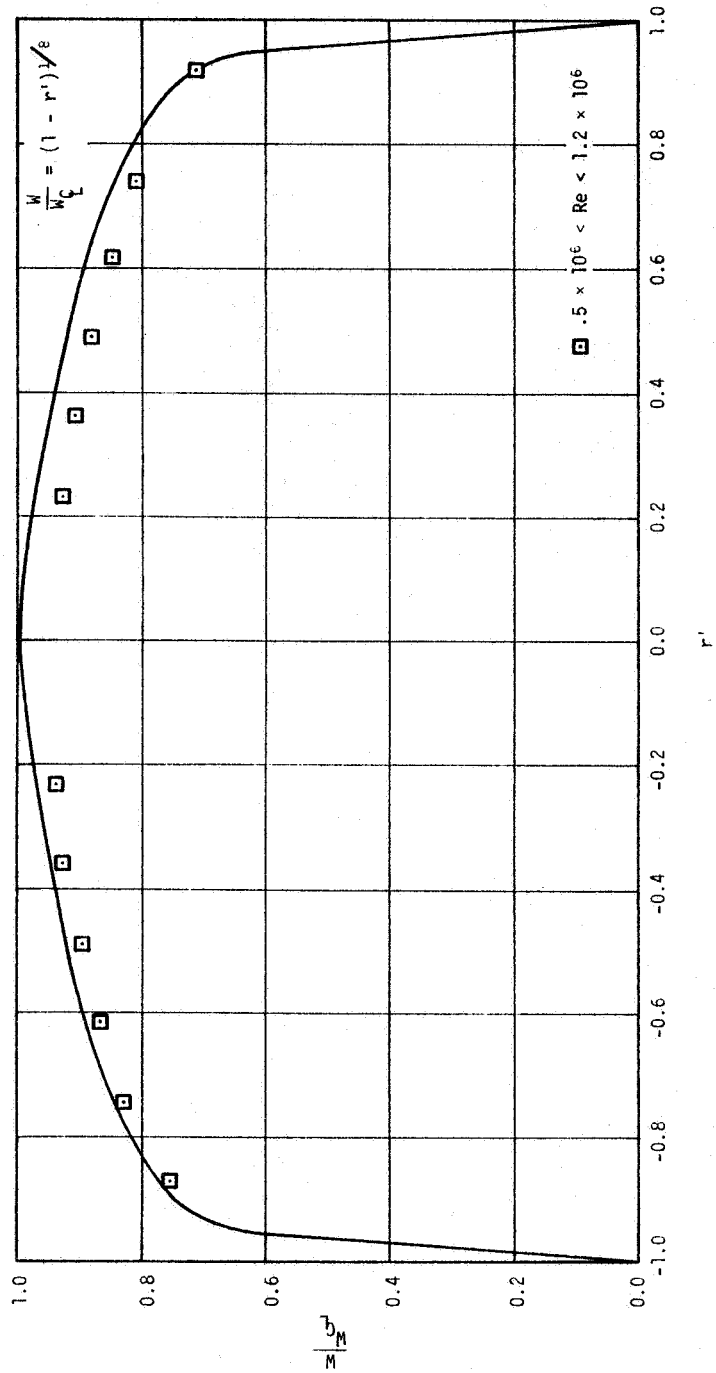


Figure 5. Velocity Traverse Upstream of Bend Compared with 1/8 Velocity Profile ($R/2a = 0.75$)

upstream. One of the important things to note from Figure 5 is that the velocity appears symmetrical about the centerline indicating the absence of upstream flow disturbances which could alter the flow field in the pipe bend test section.²⁷

The minimum pressure coefficients ($C_{p_{\min, \text{wall}}}$) measured at the inside wall of the pipe bends are shown in Figure 6 as a function of pipe Reynolds number, Re . For the four bends of largest radii of curvature ($R/2a = 2, 1.5, 1.25, 1.00$), the pressure coefficients indicate an independence of Reynolds number over the range investigated. For the bend of smallest radius of curvature ($R/2a = 0.75$) the pressure coefficient varies with Reynolds number (Figures 6 and 7) but appears to become independent of Reynolds number with values of Re greater than about 1.4×10^6 . The independence of $C_{p_{\text{wall}}}$ with Reynolds number is in accord with the relationship obtained for other bend parameters, namely the flow discharge coefficient^{15, 16} and bend excess loss coefficient.¹⁹ These results also support the conclusions reached in the analytical portion of the program.¹³ To ascertain if there were other independent variables which would affect the results, a test run was made deviating from the normal procedure. In this run the flow rate was held essentially constant and the Reynolds number was allowed to vary by the changing of the water viscosity as it became heated. These points are indicated in Figure 6 for the small radius bend. For the range of variables examined in this exploratory investigation, the pressure coefficients were indistinguishable from those of other runs.

In Figure 8 the pressure profiles over the outside and the inside of the bends are presented. The bends of largest radii of curvature yield pressure coefficients at the wall which are essentially in accord with the results of Yarnell and Nagler;²⁷ i. e., the minimum pressure occurs at a deflection angle of about 22.5 degrees and the maximum pressure at about 60 degrees. However, as the radius of curvature is reduced (Figures 8c and 8d), the point of minimum pressure shifts to

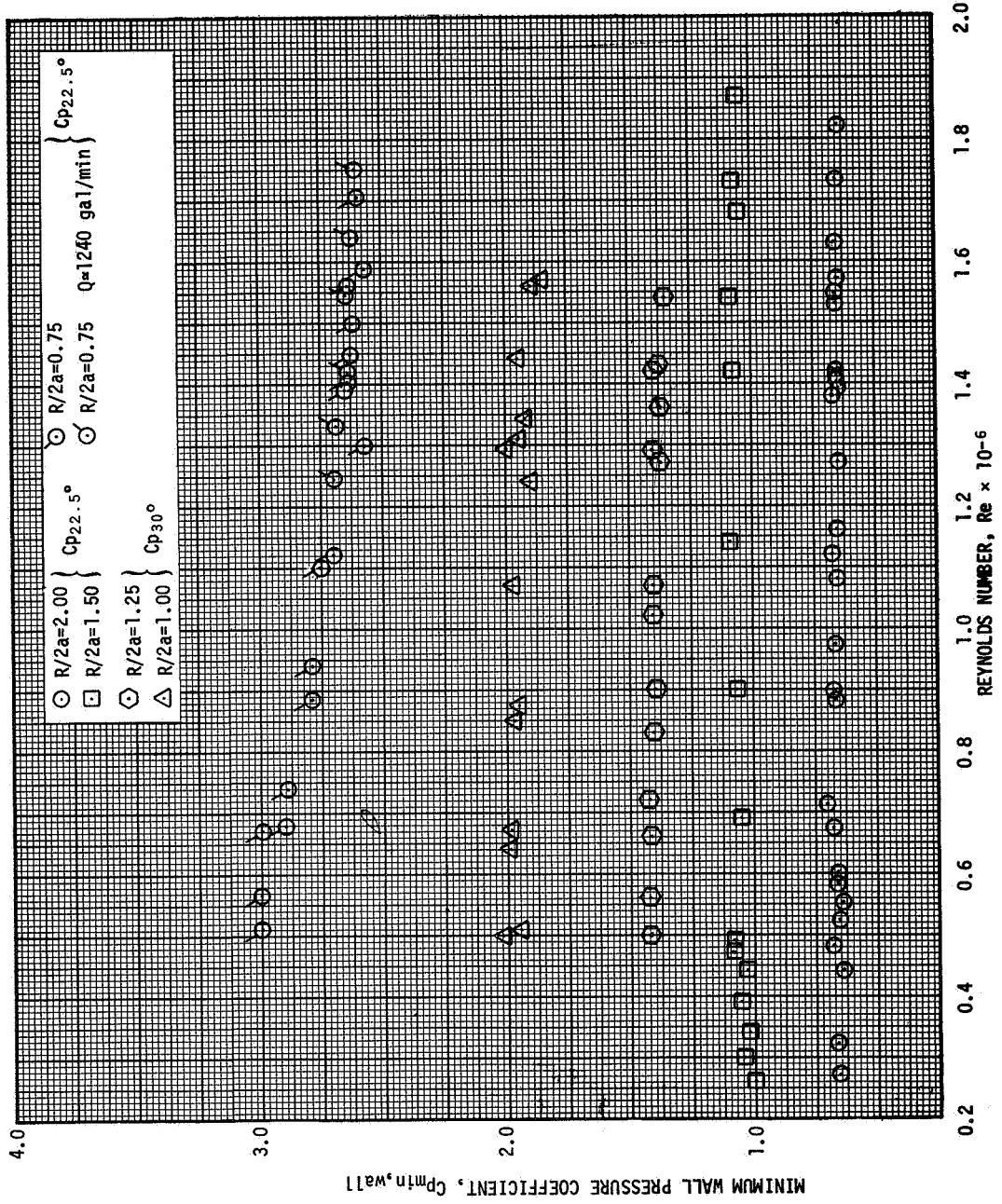


Figure 6. Variation of Minimum Wall Pressure Coefficient with Reynolds Number

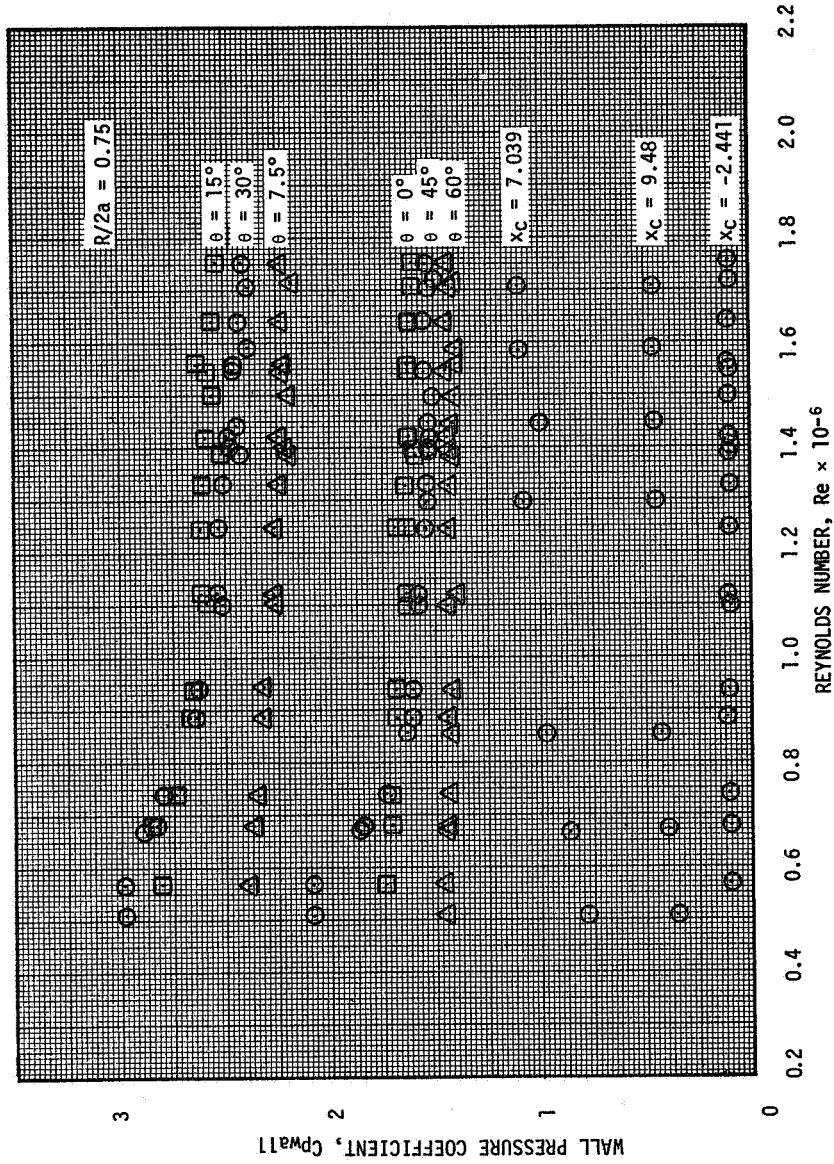


Figure 7. Variation of the Wall Pressure Coefficient with Reynolds Number ($R/2a = 0.75$)

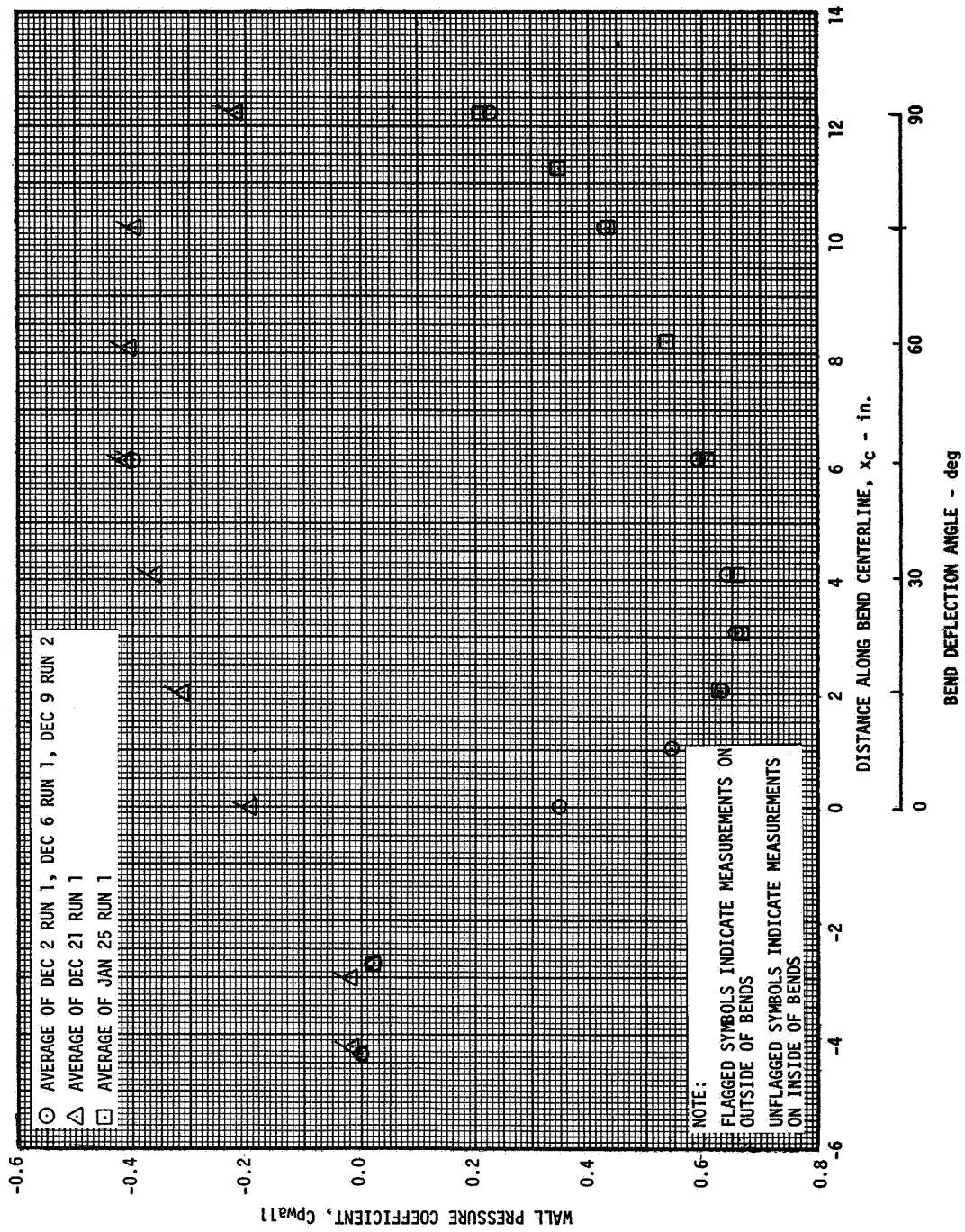


Figure 8a. Variation of Wall Pressure Coefficient with Distance Along Bend Centerline ($R/2a = 2.00$)

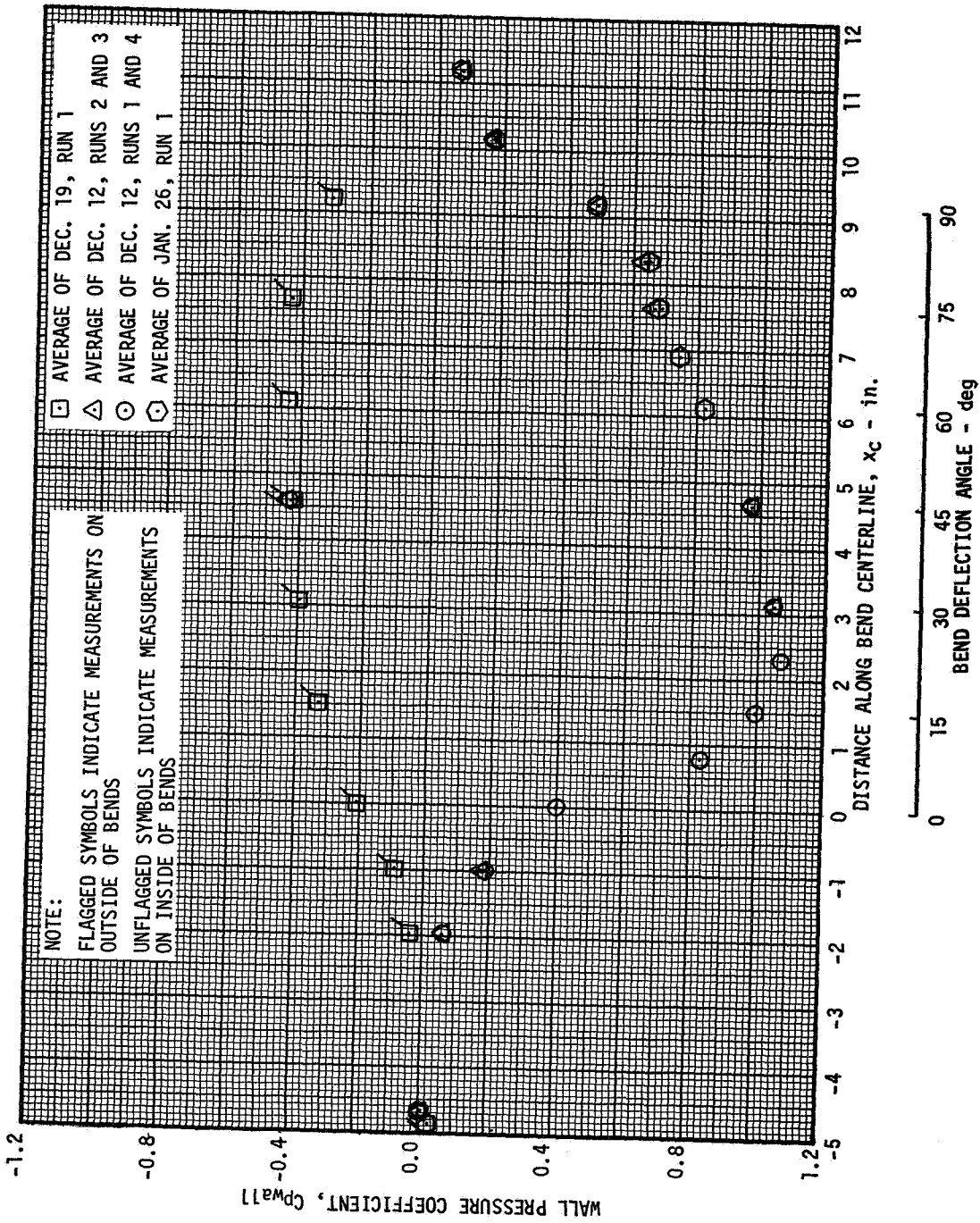


Figure 8b. Variation of Wall Pressure Coefficient with Distance Along Bend Centerline ($R/2a = 1.50$)

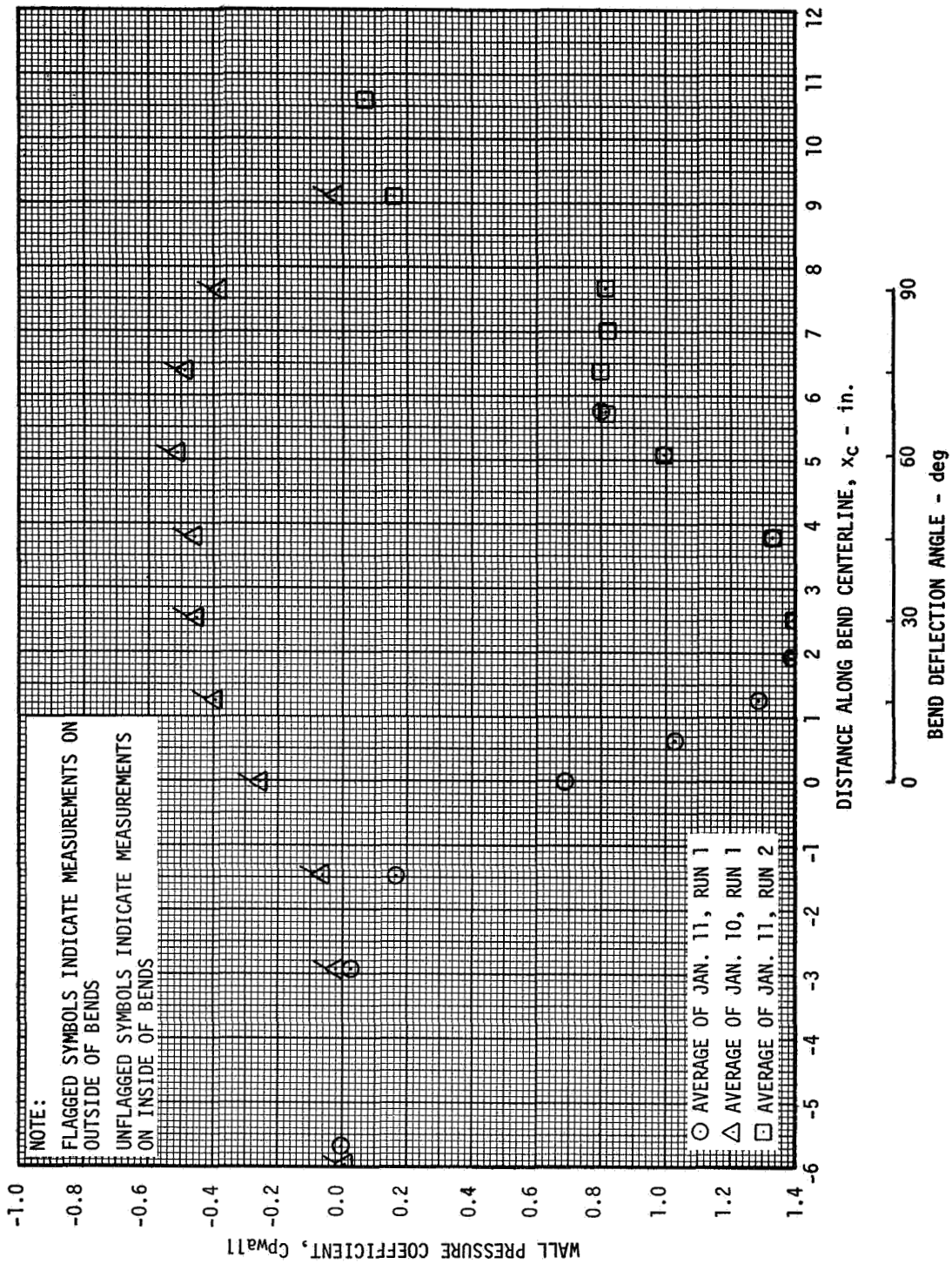


Figure 8c. Variation of Wall Pressure Coefficient with Distance Along Bend Centerline ($R/2a = 1.25$)

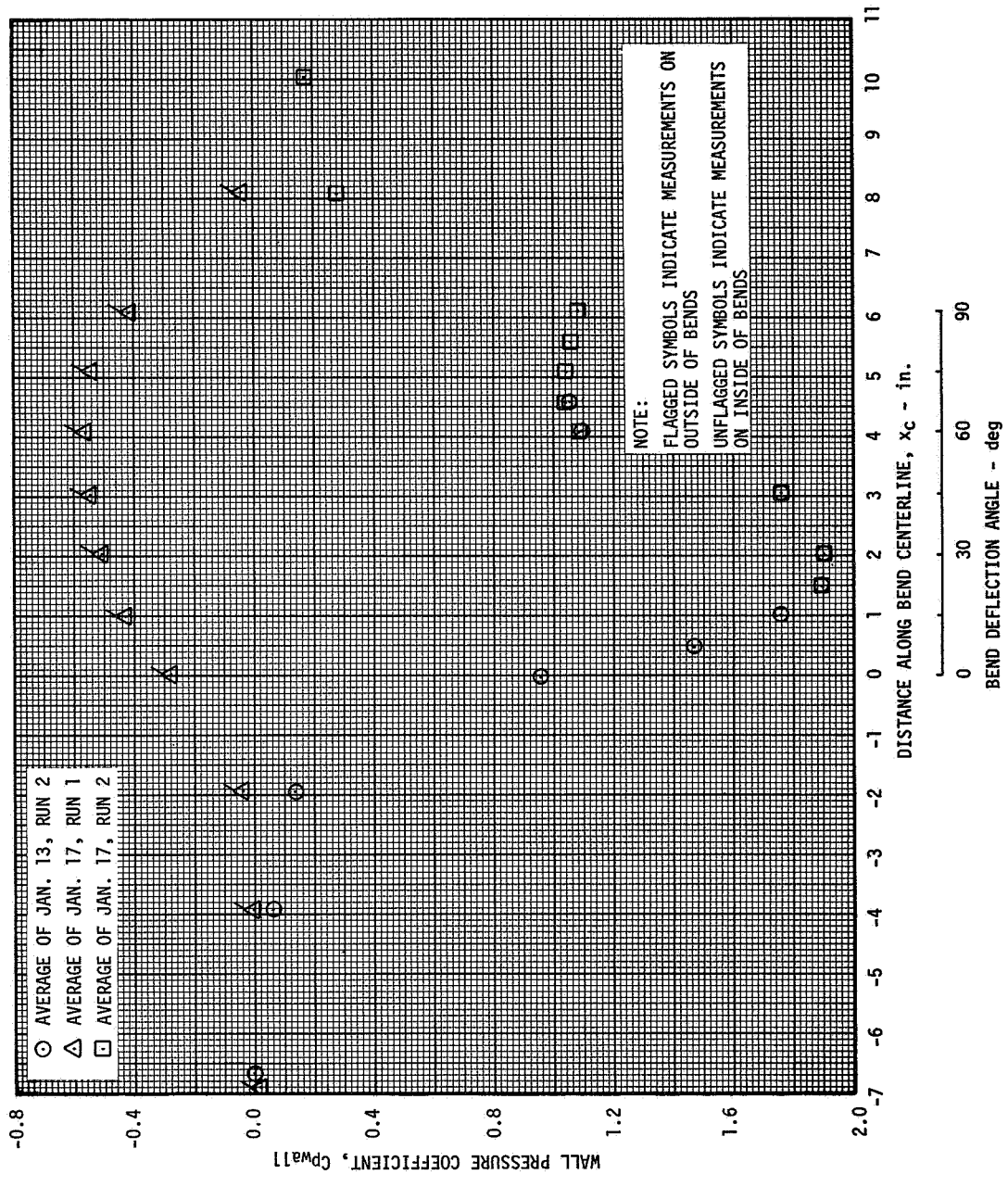


Figure 8d. Variation of Wall Pressure Coefficient with Distance Along Bend Centerline ($R/2a = 1.00$)

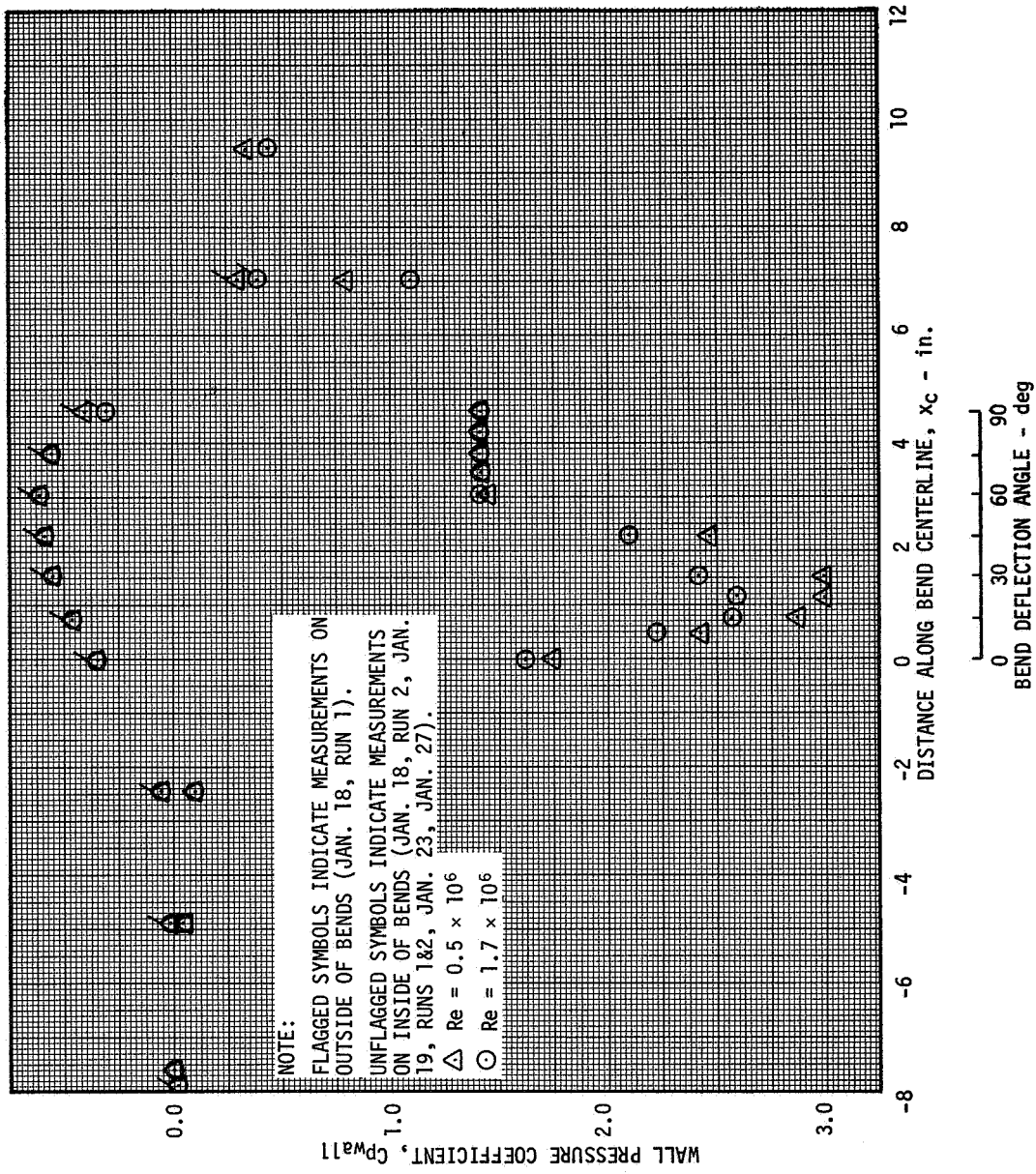


Figure 8e. Variation of Wall Pressure Coefficient with Distance Along Bend Centerline ($R/2a = 0.75$)

about 30 degrees bend deflection angle. In addition, a region of constant pressure, which is first evident for the $R/2a = 1.50$ bend, appears at the inside wall at a deflection angle of 67.5 degrees and continues to the exit of the bend. This region is interpreted to be the portion of the flow in which the boundary layer has separated; this was observed also by Weske¹⁸ with velocity traverses at the outlets of bends of various deflection angles.

The pressure variation on the bend of smallest radius of curvature (Figure 8e) deserves special mention. First, it is to be noted that the point of minimum pressure has shifted back to a deflection angle of 22.5 degrees. The region of separation, exemplified by the constant pressures, is seen to be independent of Reynolds number, which is surprising since separation is a viscosity induced phenomenon and should therefore be a function of Reynolds number. Furthermore, in the straight section downstream of the bend the higher pressures occur at the lower Reynolds numbers, whereas the reverse is true for the bend itself. The pressures in the bend would be expected to decrease rather than increase with increasing Reynolds number since a decrease in minimum pressure would represent an approach towards potential flow pressures.

Data from the Kiel probe and three-dimensional prism probe traverses are shown in Figure 9. The data are taken along a line formed by the intersection of the plane of curvature with a plane normal to the pipe centerline and located at the θ_{\min} deflection angle. Clearly the two types of total pressure measurements are in satisfactory agreement. As with the wall pressure measurements for the four larger radius bends, the data are independent of Reynolds number and the data points represent averages taken over the Reynolds number range of $0.7 \times 10^6 < Re < 1.5 \times 10^6$.

The total pressure measurements indicate that the assumption of constant total pressure is not too inexact for the central core. If the flow

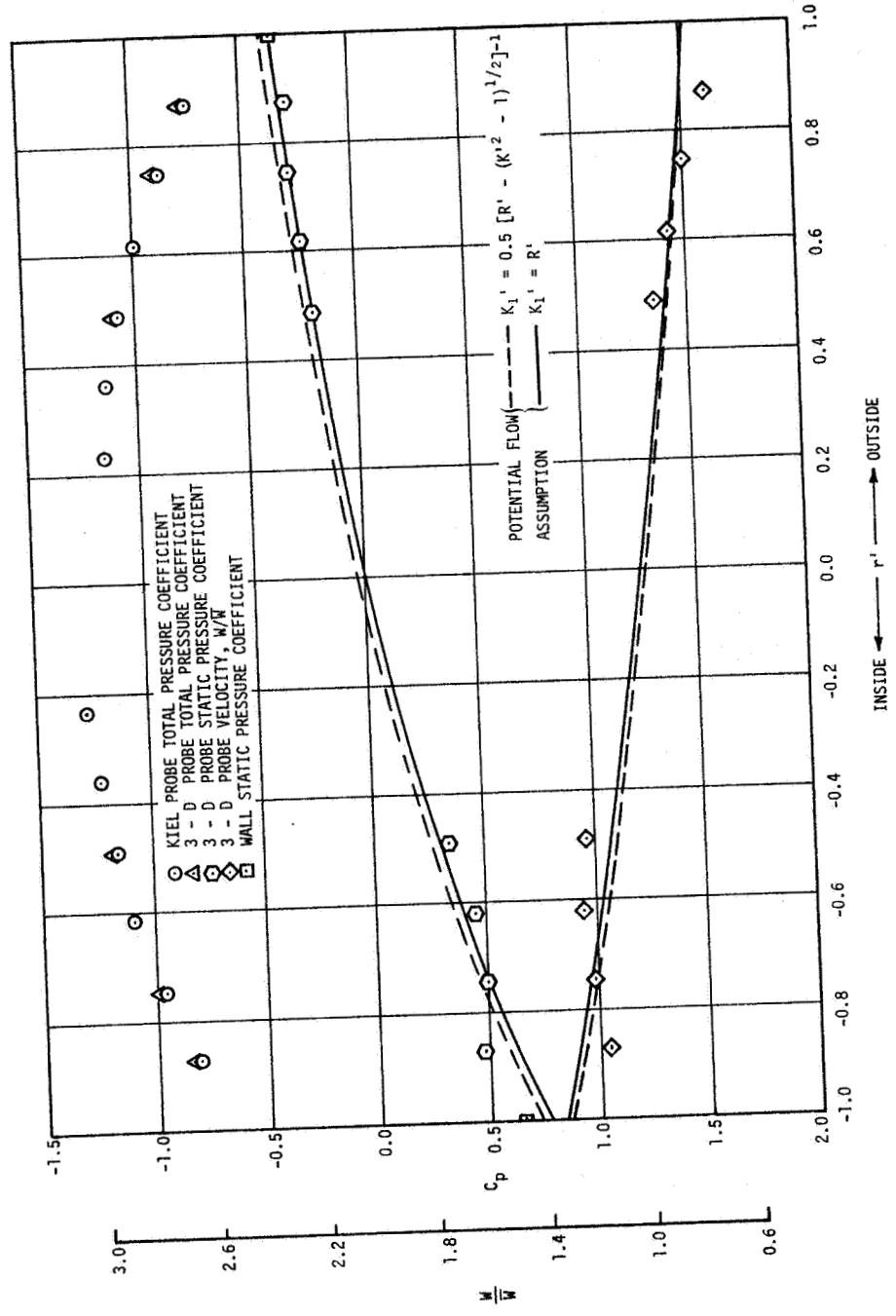


Figure 9a. Experimental Results from Probe Traverses
 ($R/2a = 2.00$, $\theta_{min} = 22.5^\circ$)

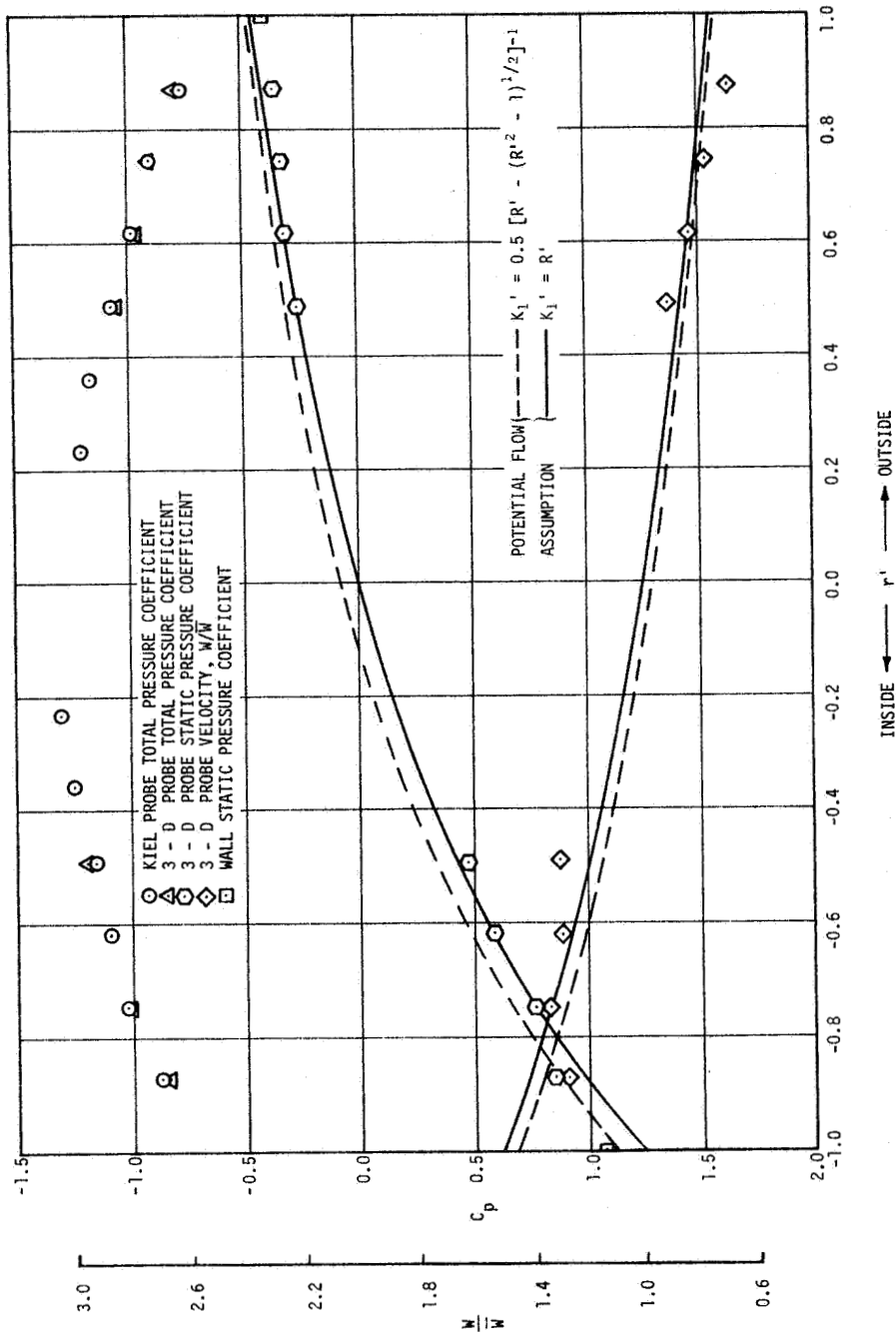


Figure 9b. Experimental Results from Probe Traverses
 ($R/2a = 1.50$, $\theta_{min} = 22.5^\circ$)

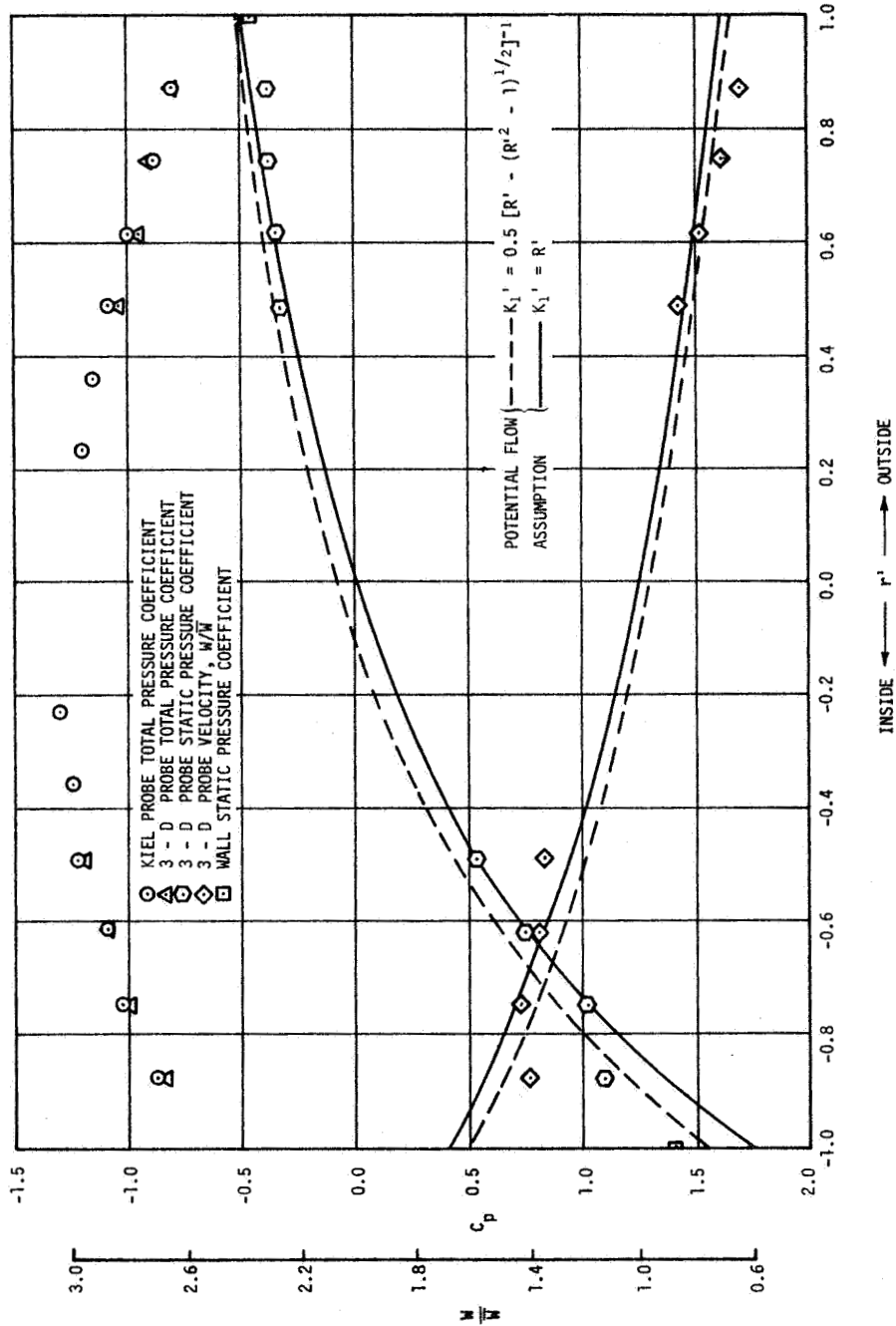


Figure 9c. Experimental Results from Probe Traverses
 ($R/2a = 1.25$, $\theta_{min} = 30^\circ$)

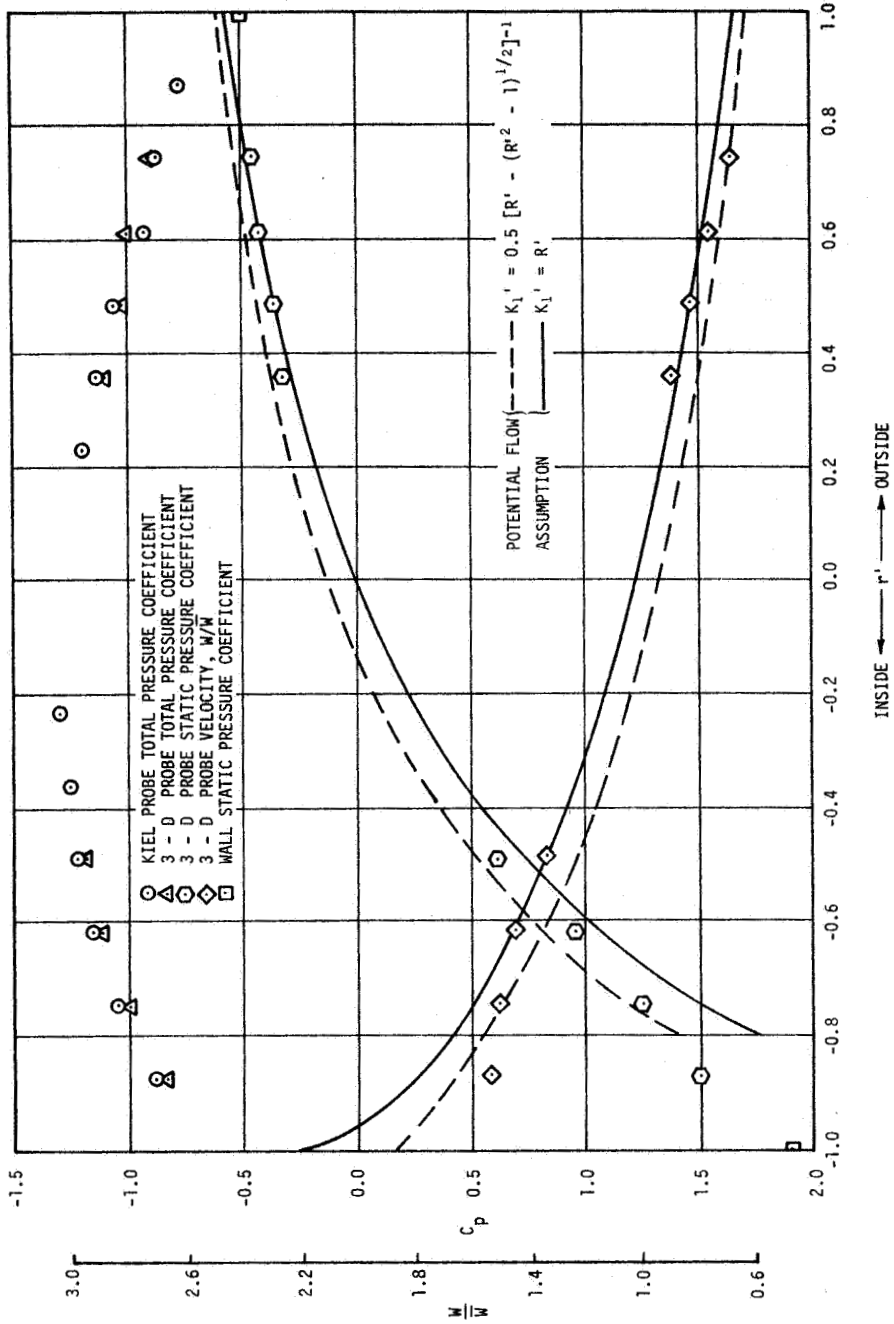


Figure 9d. Experimental Results from Probe Traverses
 ($R/2a = 1.00$, $\theta_{min} = 30^\circ$)

at the entrance to the bend is ideally assumed to be such that the core velocity is equal to the average velocity, then the total pressure coefficient would be -1.0 for constant total pressure. Actually the core velocity is greater than the average velocity at the bend entrance, thus yielding a constant total pressure coefficient less than -1.0. Close examination of the total pressure coefficient indicates that the average in the central core (which is not clearly delineated by the total pressure data) would indeed be somewhat smaller than -1.0.

The static pressure and velocity in the central core generally follow the trend expected for potential free vortex flow. In addition, the assumption of $K_1' = R'$ along with the others leading up to Equations 11 and 12 appear to be justified for the central core. The static pressure near the inside wall, however, is more closely approximated by the potential flow assumption and, because of its significance from the standpoint of cavitation, deserves special mention. From the data of Weske¹⁸ one is led to believe that the minimum pressure in the flow field should be expected not at the wall but at some small distance (called $\delta_{2,0}'$ in Reference 13) from the inside wall. This distance is in effect a measure of the thickness of the "region of eddy motion"* near the inside wall. Within the resolution of the measurement techniques, the present results indicate that the minimum pressure occurs immediately at the wall and that the pressure distribution in the region of eddy motion is a monotonically decreasing function altered by the viscous effects near the wall such that the distribution lies increasingly further from the free vortex type of pressure distribution as the inner wall is approached. The difference between the present results and those of Weske¹⁸ could lie in the fact that Weske's measurements were made at the exit planes of bends exhausting into the atmosphere.

*See Reference 13 for a definition.

Since disturbances are propagated upstream, the comparison of those measurements with the ones taken upstream of the bend exit is not entirely valid.

Figure 10 presents the measured pitch angle between the velocity vector and a vector tangent to the bend centerline. The magnitude of the angle (the positive direction indicates secondary flow from the inner to the outer walls of the bend) is a measure of the intensity of the secondary motion at the cross-sectional plane corresponding to the θ_{\min} position. As would be expected, the intensity of secondary circulation increases with decreasing bend radius. There are, however, surprisingly large pitch angles near the outer wall indicating the existence of a thin region where the r component of velocity is rapidly decelerated to zero at the wall. The data of Figure 10 are not averaged for all runs as was done previously, the scatter being primarily due to random pulsations in the test loop affecting the manometer-pressure indications.

Figure 11 presents a comparison of the measured minimum wall pressures with the results from potential flow theory. As illustrated by the measured static pressure distribution across the bend (Figure 9), the pressure measured at the wall will be greater than the potential wall pressure because of the viscous effects in the region of eddy motion at the inner wall.

Finally, Figure 12 presents the relationship between the empirical coefficient C_{wall} and the radius of curvature. The fact that the data points do not lie on a smoothly faired curve could possibly be an indication of a number of effects. First, it could be an indication of a slight installation misalignment of one of the bends or, more possibly, it could be due to normal scatter of the data and the fact that Equation 10, when solved for C_{wall} , is in the form of a difference between two terms of very

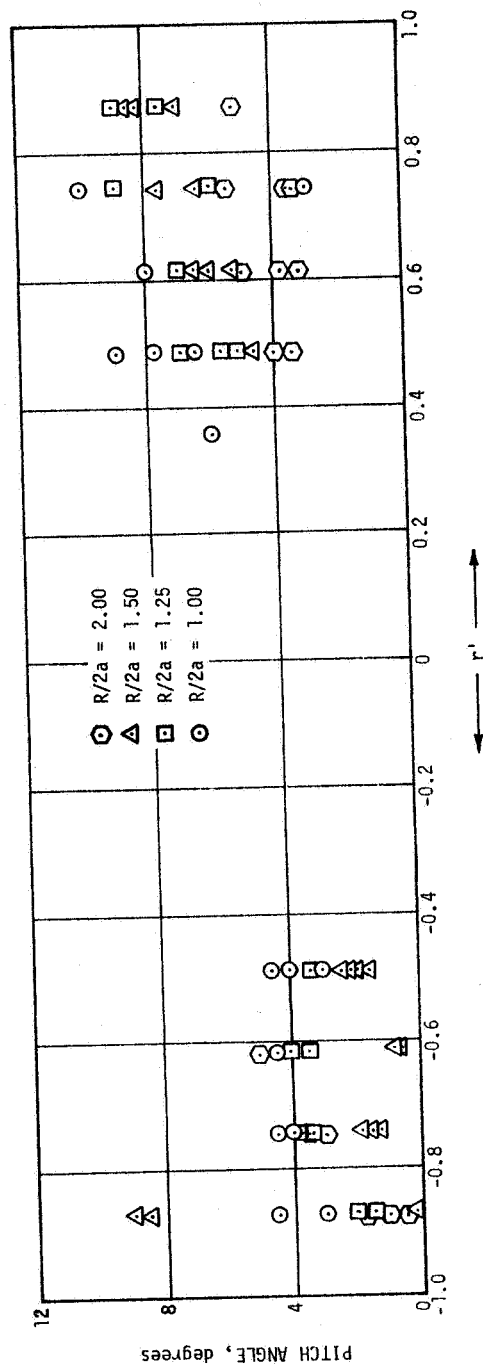
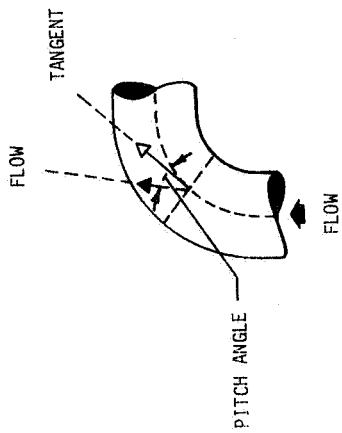


Figure 10. Flow Pitch Angles Measured Relative to a Tangent to the Bend Centerline

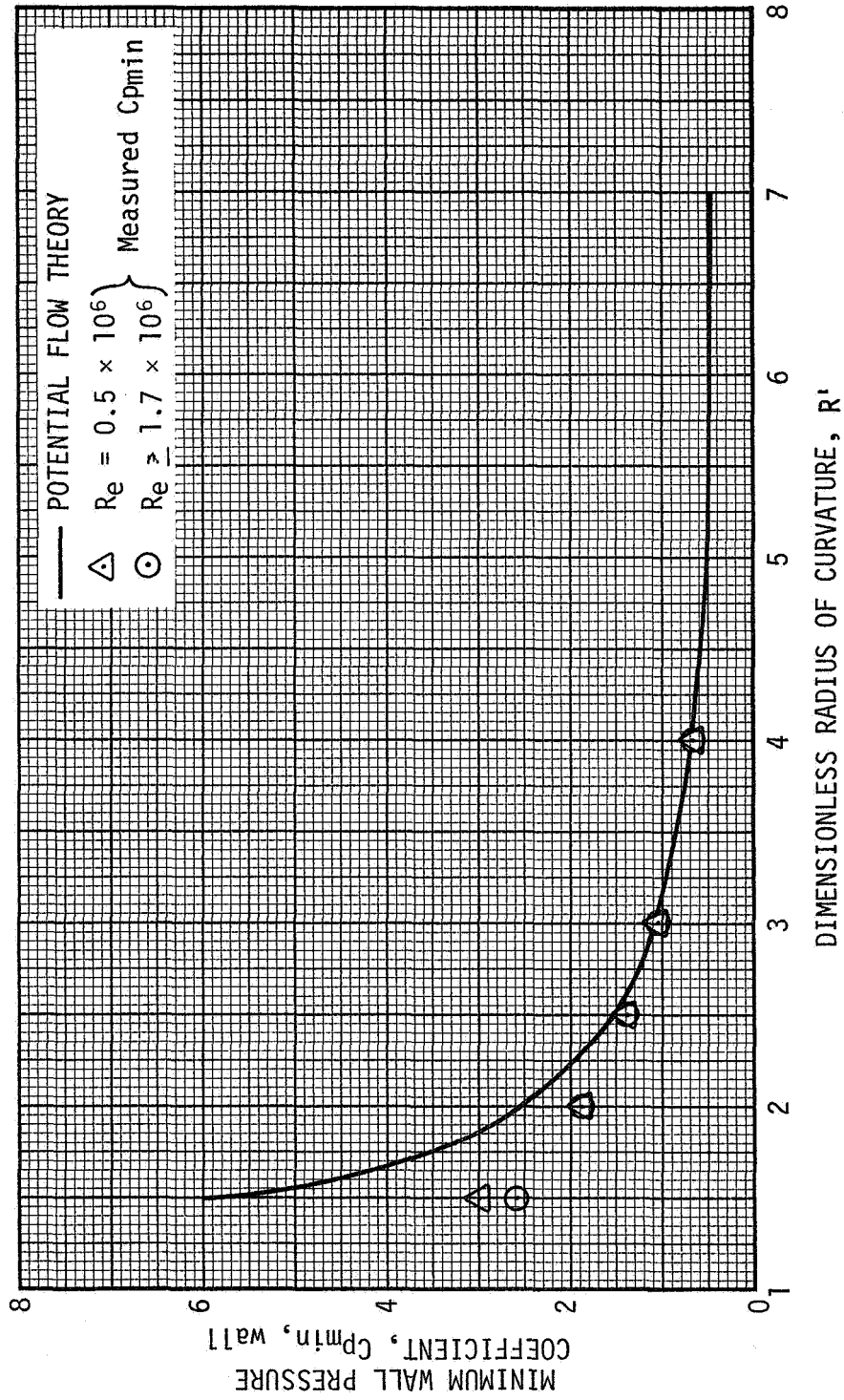


Figure 11. Comparison of Measured Minimum Wall Pressure Coefficient with Potential Flow Theory

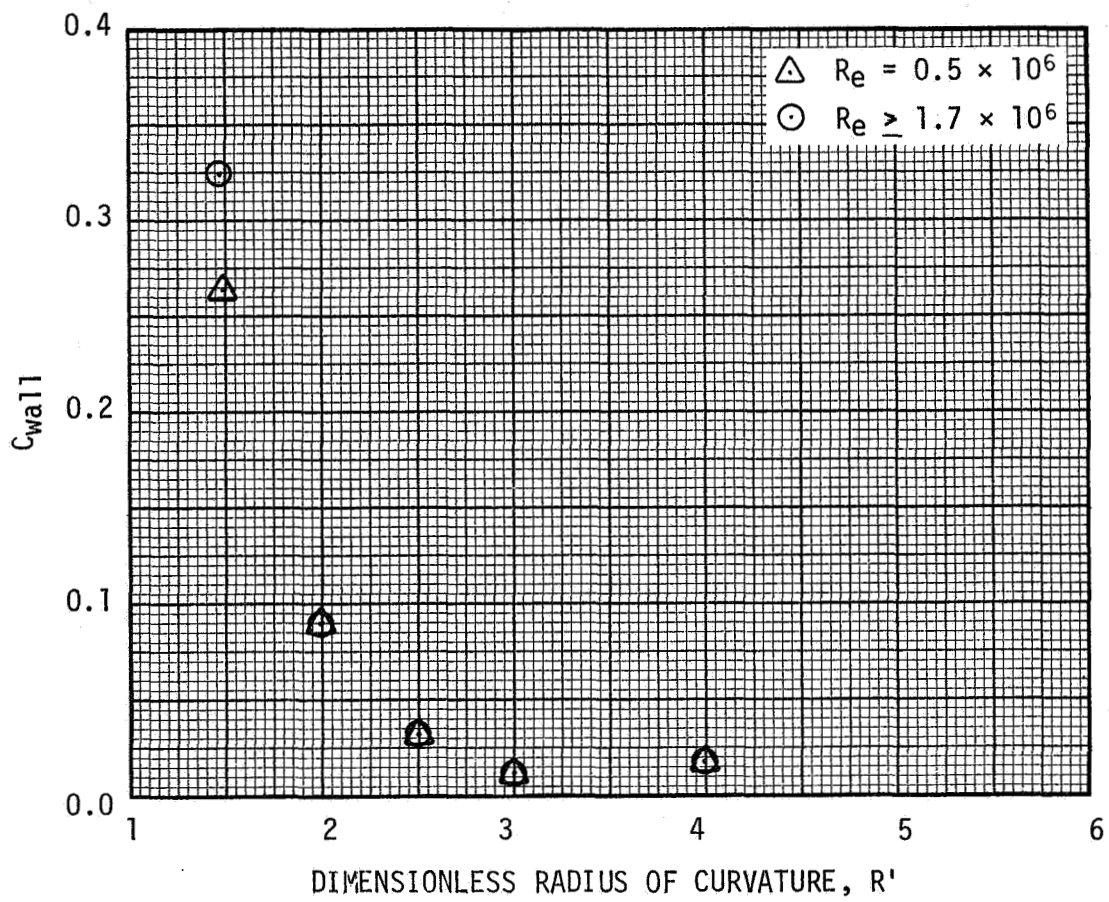


Figure 12. Variation of C_{wa11} with Radius of Curvature, R'

nearly equal magnitude. However, the values of a number of bend parameters, especially those related to the viscous effects in the bend such as loss coefficients, ¹⁹ discharge coefficients, etc., oscillate with changing radius of curvature. Since C_{wall} is an algebraic function of the average boundary layer thickness, it is quite possible that it could also experience such a relationship with radius of curvature. More measurements are needed at higher R' to establish the validity of this supposition.

CONCLUSIONS

Wall pressure measurements in the plane of curvature and velocity, total pressure, and static pressure traverses across the plane of minimum wall pressure have led to the following conclusions for 90-degree circular pipe bends.

- For a sufficiently high Reynolds number the pressure coefficients are independent of Reynolds number. The value at which the transition to a constant wall pressure coefficient takes place is $Re = 1.4 \times 10^6$ for the smallest bend radius of curvature tested ($R/2a = 0.75$). For the larger bend curvatures the transition point was not observed for the range of Reynolds numbers tested ($0.5 \times 10^6 < Re < 1.7 \times 10^6$).
- The minimum wall pressure occurs at a deflection angle of 22.5 degrees for the two largest curvatures ($R/2a = 2, 1.5$) and the smallest curvature. For the intermediate curvatures ($R/2a = 1.25, 1.00$) the minimum pressure is at 30-degree deflection angle. For all bends tested the maximum pressure on the outside wall occurs at a deflection angle of about 60 degrees.
- For bends with a radius of curvature ($R/2a$) less than 1.50 a region of constant wall pressure appears at about 67.5 degrees on the inside wall and persists to the bend exit. This region is expected to coincide with a region of separated flow.
- The minimum wall pressures at the inside of the bend are greater than that predicted from potential flow with the difference increasing for smaller bend curvatures.

- In the central core the flow variables are closely approximated by the free vortex assumption with $K_1' = R'$; however, the potential flow assumption more closely approximates the minimum static pressure.
- The minimum pressure is observed to occur at the wall.

REFERENCES

1. Stripling, L. B. and A. J. Acosta, "Cavitation in Turbopumps - Part 1", Trans. ASME, pp. 326-338, September 1962
2. Stripling, L. B. and A. J. Acosta, "Cavitation in Turbopumps - Part 2", J. Basic Eng., pp. 339-350, September 1962
3. Wood, G. M., F. H. Hartz, F. G. Hammitt, and A. Agostinelli, "Cavitation in Fluid Machinery", Am. Soc. Mech. Engrs., 1965
4. Stepanoff, A. J., "Cavitation in Centrifugal Pumps", Trans. ASME, pp. 533-552, May 1955
5. Wislicenus, G. F., "Critical Considerations on Cavitation Limits of Centrifugal and Axial-Flow Pumps", Trans. ASME, pp. 1707-1714, November 1956
6. Wislicenus, G. F., R. M. Watson, and I. J. Karassik, "Cavitation Characteristics of Centrifugal Pumps Described by Similarity Considerations", Trans. ASME, pp. 17-24, January 1939
7. Guinn, G. R., "A Review of Governing Processing and Liquid Cavitation Phenomena for Flow in Curved Ducts", Brown Engineering Company, Inc., Technical Note R-119, October 1964
8. Birkhoff, Garrett and E. H. Zarantonello, Jet Wakes and Cavities, Academic Press, Inc., New York, 1957
9. Holl, J. W. and G. F. Wislicenus, "Scale Effects on Cavitation", J. Basic Eng., pp. 385-398, September 1961
10. Sarosdy, L. R. and A. J. Acosta, "Note on Observations of Cavitation in Different Fluids", J. Basic Eng., pp. 399-400, September 1961
11. Robertson, J. M., J. H. McGinley and J. W. Holl, "On Several Laws of Cavitation Scaling", LaHouille Blanche, No. 4, pp. 550-554, September 1957
12. Holl, J. W., "An Effect of Air Content on the Occurrence of Cavitation", J. Basic Eng., pp. 941-946, December 1960
13. Guinn, G. R., "Analysis of the Flow and Minimum Pressures in Pipe Bends", Brown Engineering Company, Inc., Technical Note R-157, September 1965

14. Guinn, G. R., "An Experimental Study of the Pressure at the Walls of Ninety-Degree Pipe Bends", Brown Engineering Company, Inc., Technical Note R-231, February 1967
15. Addison, Herbert, "The Use of Pipe Bends as Flow Meters", Engineering, pp. 227-229, March 4, 1938
16. Lansford, W. M., "The Use of an Elbow in a Pipe Line for Determining the Rate of Flow in the Pipe", University of Illinois, Bulletin No. 289, December, 1936
17. Murdock, J. W. and D. Gregory, Jr., "Elbow Flow Meter Investigation", Naval Boiler and Turbine Laboratory Project I-184, December 10, 1962
18. Weske, J. R., "Experimental Investigation of Velocity Distributions Downstream of Single Duct Bends", National Advisory Committee for Aeronautics, Technical Note 1471, January 1948
19. Anderson, A. C. and L. C. Straub, "Hydraulics of Conduit Bends", St. Antony Falls Hydraulic Laboratory, University of Minnesota, Bulletin No. 1, December 1948
20. Adler, V. M., "Stromung in gekrummten Rohren", Z. Angew. Math. Mech., Ingenieurwissenschaftliche Forschungsarbeiten Band 14, Heft 5, pp. 17-275 (1934)
21. Barua, S. N., "On Secondary Flow in Stationary Curved Pipes", Quart. J. Mech. Appl. Math., Vol. XVI, Pt. 1, pp. 61-77 (1963)
22. Barua, S. N., "Secondary Flow in a Stationary Curved Pipe", Fluid Motion Subcommittee, Aeronautical Research Council, F. M. 2162, November 1954 (AD141862)
23. Weske, J. R. "Investigations of the Flow in Curved Ducts at Large Reynolds Numbers", J. Appl. Mech., pp. 344-348, December 1948
24. Ito, Hidesato, "Friction Factors for Turbulent Flow in Curved Pipes", J. Basic Eng., pp. 123-134, June 1959
25. Ito, Hidesato, "On the Pressure Losses for Turbulent Flow in Smooth Pipe Bends (Report 2)", Reports of the Institute of High Speed Mechanics, Tohoku University, Vol. 7, 1956

26. Eckert, E. R. G. and R. M. Drake, Jr., Heat and Mass Transfer, McGraw-Hill Book Company, Inc., New York, 1959
27. Schlichting, Hermann, Boundary Layer Theory, McGraw-Hill Book Company, Inc., New York, Ed. 4, 1960
28. Yarnell, D. L. and F. A. Nagler, "Flow of Water Around Bends in Pipes", Am. Soc. Civil Engrs. 100, pp. 1018-1043 (1935)

DOCUMENT CONTROL DATA - R&D

(Security classification of title, body of abstract and indexing annotation must be entered when the overall report is classified)

1. ORIGINATING ACTIVITY (Corporate author) Research Laboratories Brown Engineering Company, Inc. Huntsville, Alabama		2a. REPORT SECURITY CLASSIFICATION Unclassified	
		2b. GROUP N/A	
3. REPORT TITLE "An Experimental Study of the Flow Variables at the Minimum Pressure Station of Ninety-Degree Pipe Bends"			
4. DESCRIPTIVE NOTES (Type of report and inclusive dates) Technical Note R-243, November 1967			
5. AUTHOR(S) (Last name, first name, initial) Guinn, Dr. G. R.; and Stricklin, G. P.			
6. REPORT DATE November 1967		7a. TOTAL NO. OF PAGES 56	7b. NO. OF REFS 28
8a. CONTRACT OR GRANT NO. NAS8-20073		9a. ORIGINATOR'S REPORT NUMBER(S) TN RL-243	
b. PROJECT NO. N/A		9b. OTHER REPORT NO(S) (Any other numbers that may be assigned this report) None	
c.			
d.			
10. AVAILABILITY/LIMITATION NOTICES None			
11. SUPPLEMENTARY NOTES None		12. SPONSORING MILITARY ACTIVITY Propulsion and Vehicle Engineering Lab. Marshall Space Flight Center NASA	
13. ABSTRACT To support liquid cavitation studies, flow variables were measured which relate to the minimum pressure in 90-degree circular pipe bends. All of the bends investigated were nominally 4 inches in diameter and had ratios of curvature radius to pipe diameter of 2.00, 1.50, 1.25, 1.00, and 0.75. Water was used as the test medium and the Reynolds number ranged from 2.5×10^5 to 1.8×10^6 . To locate the minimum wall pressure, static pressures were first measured at the inner and outer walls in the plane of curvature. The minimum wall pressure was found to occur between 22.5 degrees and 30 degrees deflection angle along the inside wall. Velocity and pressure traverses were then made across the bend at the position of minimum pressure. The total pressure was found to be roughly uniform in the central core and the velocity profile was found to correspond generally to that for free vortex flow. It was found that minimum pressures in the bend could be approximated by free vortex flow; however, the predicted values will be conservative, e. g., low, when viewed from the standpoint			14. KEY WORDS Pipe bends Curved ducts Cavitation

of cavitation.